CHALMERS

Brake system and rear suspension for an electric ultra light vehicle

An investigation into suspension- and brake system-setups

Master's thesis in Automotive Engineering

ANDREAS JOHANSSON
MAGNUS NILSSON

Department of Product and Production Development
Division of Product Development
CHALMERS UNIVERSITY OF TECHNOLOGY
Gothenburg, Sweden 2011
Master's thesis 2011

MASTER'S THESIS IN AUTOMOTIVE ENGINEERING

Brake system and rear suspension for an electric ultra light vehicle

An investigation into suspension- and brake system-setups

ANDREAS JOHANSSON
MAGNUS NILSSON

Department of Product and Production Development
Division of Product Development
CHALMERS UNIVERSITY OF TECHNOLOGY

Gothenburg, Sweden 2011

Brake system and rear suspension for an electric ultra light vehicle
An investigation into suspension- and brake system-setups
ANDREAS JOHANSSON
MAGNUS NILSSON

Master's thesis 2011
Department of Product and Production Development
Division of Product Development
Chalmers University of Technology
SE-412 96 Gothenburg
Sweden
Telephone: +46 (0)31-772 1000

Cover:

Chalmers Reproservice
Gothenburg, Sweden 2011

Brake system and rear suspension for an electric ultra light vehicle
An investigation into suspension- and brake system-setups
Master's thesis in Automotive Engineering
ANDREAS JOHANSSON
MAGNUS NILSSON
Department of Product and Production Development
Division of Product Development
Chalmers University of Technology

Abstract

Since the demands on decreased energy consumption and pollution has increased significantly in the 21st century, most vehicle manufacturers have spent alot of money and time to improve their vehicles in this aspect. While many improvements are made on drivetrains and vehicle aerodynamics the factor that ultimatley has the largest influence on energy consumption at low speeds is the curbweight of the vehicle. Most attempts to reduce the weight of the vehicle has been done to improve performance and not to reduce the fuel consumption.

In the beginning of 2010 the company Clean Motion AB started developing a novel vehicle concept for urban transportation based on an advanced composite body with an electric drivetrain. The vehicle is a covered three wheeled moped, capable of transporting three people, and will comply with the European L2e-standard.

The scope of this report is to give recommendations on how to design a brake system and rear suspension for this vehicle. The brake system must fulfill the legal requirements according to the European L2e-standard. The main issue with developing a brake system for this vehicle is that the occupants of the vehicle may weigh as much as 150% of the vehicles curbweight. This means that the forces required to ensure a controlled deceleration varies greatly depending on the number of passengers.

The main problems with developing a suspension system are also weight-related. The loads on the rear wheels vary greatly depending on the number of passengers, and the suspension must regardless of the load behave predictably and ensure good comfort. Since the vehicle has the three-wheel configuration it is also important that the suspension minimizes any amount of roll that is created due to lateral acceleration in order to reduce the risk of the vehicle rolling over. Both the brake system and the suspension must also have a low weight and a low cost.

Based on the results from both calculations and physical testing of prototype vehicles two brake systems fulfilling the requirements were composed. The first consist of a combined brake system with single brake discs on all wheels. The front caliper is hydraulic and the rear calipers are both hydraulicly and mechanically actuated. The second consists of a single disc with hydraulic caliper as front brake and a single disc with mechanical brake caliper for each rear wheel. The front and rear brakes are actuated by separate brake levers. The rear brakes also functions as parking brakes, hence the mechanical actuation. Both systems are assisted by the electric motors which can be used as generators for braking. The final decision is made with regards to availability of components and cost.

The recommended suspension system is a rubber suspension axle which uses rubber rods as both spring and damper. This gives a cheap suspension system which can be fully integrated into the chassis. Other advantages is that the construction can be made light and it also has a noise reducing property.

Keywords: Brake system, Suspension, Rubber suspension axle, Torsion suspension, Electric Ultra Light Vehicle, European L2e category

Preface

This report covers the master thesis on the development of a brake system and a rear suspension system for an ultralight electric vehicle. This master thesis was performed during the spring semester of 2011 for Clean Motion AB in collaboration with the department of Product and Production Development at Chalmers University of Technology.

Acknowledgements

We would like to thank the following people for their invaluable contributions to this master thesis;

Göran Brännare	Division of Product Development, Chalmers University of Technology
Peter Helmroth	Clean Motion AB
Hans Folkesson	Clean Motion AB
Göran Folkesson	Clean Motion AB
Prof. Larsgunnar Nilsson	Division of Solid Mechanics, Linköping University
Nils Nilsson	Technician, Chalmers University of Technology
Jan Bragee	Research Engineer, Chalmers University of Technology

Andreas Johansson
Magnus Nilsson
Gothenburg 27 th May 2011

Nomenclature

ATV	All Terrain Vehicle
CAD	Computer Aided Design
CM	Clean Motion AB
COG	Center Of Gravity
EULV	Electric Ultra Light Vehicle
EV	Electric Vehicle
P1A	Prototype 1A
P1B	Prototype 1B
P1C	Prototype 1C
P1D	Prototype 1D
PT	Physical testing
SC	Static calculations

Contents

List of Figures

List of Tables

1 Introduction

The worlds energy consumption is increasing. As the worlds population increases and the overall standard of life improves, the sustainability of all current energy-systems will also have to improve. With fossil fuel resources depleting it is vital to find new energy sources and more efficient ways to use this energy. The demands on the vehicle industry are increasing and political incentives are in certain areas promoting new and more energy-efficient vehicles. The vehicle industry is constantly working on reducing the fuel consumption of the combustion engine while developing new technologies for propulsion such as electric and hybrid vehicles.

The problem is that even though the public has become more aware about the negative consequences of consumption of fossil fuels there are still consumer satisfaction issues which needs to be adressed before electric vehicles will be suitable for large scale deployment. Since the average consumer is not willing, or able, to give up the performance of the combustion vehicle the power of the engine and the weight of the car remains essentially the same. This is especially bad for vehicles which are mainly used in urban areas where the main contributing factor to fuel consumption is the weight of the vehicle.

One of the main drawbacks of electric vehicles, when it comes to performance, is range. Most electric vehicles do not have a depleting range which make them suitable for anything other then commutor trips. And even if most consumers could manage their daily commute with an EV, people need a more versatile vehicle. A vehicle that is both capable of transporting them shorter distances, for example to work, and larger distances, i.e. on vacation.

This point leads to the next big problem, recharging. Even if the range of an EV can be improved, there is still the problem of recharging time. While a combustion vehicle can be refueled at a petrol pump in under 5 minutes, one of the best current EVs, the Tesla Roadster, can be charged at a maximum power of 16.8 kW, which is equal to a charging rate of 56 miles, approximatley 90 km, range per hour at max power[**TM**].

1.1 Background

The company Clean Motion AB is developing an electric ultralight vehicle for use in urban areas. The vehicle is a covered three wheeler with electric drive and a range of 60 km. The vehicle will be able to transport three people, including driver, and will have a curbweight of approximately 120 kg. It will be powered by two hub-motors with a maximum power output of 1.5-2 kW each. Since statistics show that most people travel an average distance of approximately 42 kilometers every day [**Inrets**] this vehicle could be used as a commutor vehicle or be a substitute for owning a second car. Certain models of this vehicle could also be used as light cargo transports and since it is fully electric it can be used indoors without affecting the quality of the air.

Before the goal product is developed a number of early stage vehicles will be produced and sold in order to be able to fund continued development and recieve input from users. The results and conclusions from this master thesis will serve as a guide for what systems to use for these vehicles.

CM have developed two prototype chassis for exhibition and testing purposes. These prototype chassis have been altered during the master thesis with different combinations of brake- and suspension systems. These combinations are denoted as P1A, P1B, P1C and P1D. The first, P1A, was equipped with a single hub-motor on the front wheel and a rubber suspension axle. The braking system consisted of a front single brake disc and caliper. P1A was then converted into P1B, which meant that the rear suspension was changed into a shockabsorber setup and two rear hub-motors was installed. All of these components came from an existing EV, an EVT-Trike [**EVT**], and the suspension geometry was kept identical. The braking system was also kept identical which meant that a mechanically actuated drum brake was installed on the front wheel and a single brake disc with caliper on each rear wheel. P1C is a separate body with a rubber suspension axle and two rear hub-motors. P1B was finally converted into P1D which kept the brake and propulsion system of P1B but got an rubber suspension axle similar to that of P1C. Further specifications and pictures are found in table 6.2.1 thru 6.2.4 and figure 6.2.1 and 6.2.2 in Appendix A.

1.2 Problem definition

The project task is to develop a suitable brake system and propose a suitable rear suspension setup for the vehicle described in section 1.1. The brake system must consist of standard components while fulfilling the legal requirements for a vehicle of the European L2e category. The results for the suspension setup should include two different concepts. One with an ordinary shockabsorber and one utilizing a rubber suspension axle where rubber rods are used instead of spring and damper.The suspension should give the vehicle predictable behaviour while at the same time giving the driver and the passengers a comfortable ride. Both brakes and suspension must also be optimized with respect to weight and cost.

1.3 Delimitations

The project should only lead to recommendations regarding brakes and rear suspension. There will be no manufacturing and no tests performed on a completed system. The design of the suspension system must be adapted to the vehicle chassis and the electric motors chosen for the driveline. Table 1.3.1 shows a list of dimensioning factors that have been given by Clean Motion AB.

Table 1.3.1: Dimensioning factors

Factor	Denotation	Value
Maximum vertical acceleration	a_z	2.5 g
Maximum longitudinal acceleration	a_x	0.2 g
Maximum lateral acceleration	a_y	0.5 g
Maximum total mass	m_{tot}	385 kg
Driver nominal weight	m_d	75 kg
Passenger nominal weight	m_p	75 kg
Luggage weight	m_l	10 kg
Wheelbase	L	1.96 m
Trackwidth	t_w	1 m
Wheel radius	r_w	0.215 m

2 Theory

This chapter contains the various theory sections that needs to be considered in order to develop suitable brake- and suspension-systems for the CM EULV. The current legal requirements, different brakesystem- and suspensionsystem-setups are discussed and compared with regards to section 1.2. Please note that the legal requirements, section 2.1, should be viewed as a summary applicable to this thesis, and does not contain all of the regulations and requirements.

2.1 Legal requirements

In order for any two or three-wheel motor vehicles to be used on public roads in the European Union, they must be approved according to Council Directive 92/61/EEC of 30 June 1992 [**9261**] which relates to the type-approval of these vehicles. This directive was amended by Directive 2000/7/EC of the European Parliament and of the Council of 20 March 2000 [**007**] and by Directive 2002/24/EC of the European Parliament and of the Council of 18 March 2002 [**0224**].

The directives that specifically adresses the brake system are Council Directive 93/14/EEC of 5th April 1993 [**9314**] with the amendment of the Commision Directive 2006/27/EC of 3 March 2006 [**0627**]. These directives contains the regulations for all two- or three-wheel motor vehicles. It is therefore important to discern which regulations apply to the different categories of vehicles. These categories are listed in table 2.1.1.

In short, a moped is defined as a two- or three-wheel vehicle fitted with an engine, with a cylinder capacity not exceeding 50 cm^3 if of the internal combustion type, and having a maximum design speed of not more than 45 km/h [**9261**].

The following paragraph contains a draft of the definitions, construction- and fitting-requirements and brake tests described in Council Directive 93/14/EEC [**9314**] and Commision Directive 2006/27/EC [**0627**]. These definitions needs to be well understood and followed when developing a vehicle of the L2e category.

Table 2.1.1: European L-vehicle categories

Category	Vehicle
L1e	Moped
L2e	Three-wheel moped
L3e	Motorcycle
L4e	Motorcycle with sidecart
L5e	Three-wheel motorcycle
L6e	Light Quadricycles
L7e	Heavy Quadricycles

Definitions

Braking device:
means the combination of parts other than the engine whose function is to progressively reduce the speed of a moving vehicle or to bring it to a halt, or to keep it stationary if it is already halted. The device consists of the control, the transmission and the brake proper.

Control:
means the part actuated directly by the driver to furnish to the transmission the energy required for braking, or for controlling it. This energy may be the muscular energy of the driver, or energy of another source controlled by the driver, or a combination of these various kinds of energy.

Transmission:
means the combination of components comprised between the control and the brakes and linking them functionally. Where the braking power is derived from or assisted by a source of energy independent of the driver but controlled by him, the reserve of energy in the device is likewise part of the transmission.

Brake:
means the parts of the braking device in which the forces opposing the movement of the vehicle are developed.

Combined braking system:
means, in the case of three-wheel mopeds and tricycles, a braking device which operates on all the wheels.

Maximum design speed:
means the speed which the vehicle cannot exceed, on the level and without undue external influence, taking into account any special limitations imposed on the design and construction of the vehicle.

Maximum mass:
means the maximum mass stated by the vehicle manufacturer to be technically permissible (this mass may be greater than the permissible maximum mass laid down by the national administration).

Unladen vehicle:
means the vehicle alone, as submitted for the tests, plus the driver alone and any necessary test equipment or instrumentation. Note that for all instances other then braking, unladen vehicle implies curbweight.

Laden vehicle:
means, except where otherwise stated, a vehicle so laden as to attain its maximum mass.

Service braking:
The service braking must make it possible to control the movement of the vehicle and to halt it safely, speedily and effectively, whatever its speed and load, on any up or down gradient. It must be possible to graduate this braking action. The driver must be able to achieve this braking action from his driving seat without removing his hands from the steering control.

Parking brake:
The parking brake must make it possible to hold the vehicle stationary on up or down gradients even in the absence of the driver, the working parts being then held in the locked position by a purely mechanical device. The driver must be able to achieve this braking action from his driving seat. The parking brake must also act on at least all wheels on one axle.

Characteristics of braking devices:
Every three-wheel moped must be equipped with either two independent service braking devices which

together actuate the brakes on all of the wheels, or a service braking device which operates on all the wheels, and a secondary (emergency) braking device which may be the parking brake. In addition, every three-wheel moped must be equipped with a parking braking device acting on the wheel or wheels of at least one axle. The parking braking device, which may be one of the two independent service braking devices , must be independent of the device acting on the other axle or axles.

The performance prescribed for braking devices shall be based on the stopping distance and/or the mean fully developed deceleration. The performance of a braking device shall be determined by measuring the stopping distance in relation to the initial speed of the vehicle and/or measuring the mean fully developed deceleration during the test. The stopping distance shall be the distance covered by the vehicle from the moment when the driver begins to actuate the control of the braking system until the moment when the vehicle stops; the initial vehicle speed, v_1, shall be the speed at the moment when the driver begins to actuate the control of the braking system; the initial speed shall not be less than 98 % of the prescribed speed for the test in question. The mean fully developed deceleration, d_m, shall be calculated as the deceleration averaged with respect to distance over the interval v_b to v_e according to equation 2.1.1.

$$d_m = \frac{v_b^2 v_e^2}{25,92(s_e - s_b)} \tag{2.1.1}$$

Where:

d_m	=	mean fully developed deceleration in m/s^2
v_1	=	initial vehicle speed in km/h
v_b	=	vehicle speed at 0,8v_1 in km/h
v_e	=	vehicle speed at 0,1v_1 in km/h
s_b	=	distance travelled between v_1 and v_b in metres
s_e	=	distance travelled between v_1 and v_e in metres

The speed and distance shall be determined using instrumentation having an accuracy of ± 1 % at the prescribed speed for the test. The mean fully developed deceleration may be determined by other methods than the measurement of speed and distance; in this case, the accuracy of the d_m shall be within ± 3 %. The vehicle's condition as regards its mass must be as prescribed for each type of test and must be specified in the test report. The test must be carried out at the speed and in the manner prescribed for each type of test: if the maximum speed of the vehicle does not conform to the speed prescribed, the test must be carried out under the special alternative conditions provided. The prescribed performance must be obtained without locking of the wheel(s), without deviation of the vehicle from its course, and without any abnormal vibration. During the tests the force applied to the brake control in order to obtain the prescribed performance must not exceed the maximum laid down for the test vehicle's category.

There are four different types of tests that are applicable to two- or three-wheel motor vehicles. These tests are listed in table 2.1.2.

Table 2.1.2: Table of brake tests

Test	Description
Type-0	Test with engine disconnected
Type-0	Test with engine connected for motorcycles (with or without sidecar) and tricycles
Type-0	Test with engine disconnected: with wet brakes
Type-1	Tests brake-fatigue, a series of stops

At the start of any test or any series of tests the tires must be cold and at the pressure prescribed for the load actually borne by the wheels when the vehicle is stationary. The vehicle must be loaded, when required to be tested in the laden condition, with the load distributed in accordance with the manufacturer's prescription. For all the type-0 tests the brakes must be cold. A brake is deemed to be cold when the temperature measured on the disc or on the outside of the drum is less than 100°C. For the L2e-category and other three wheeled vehicles the type-0 tests with engine connected and wet brakes are omitted. If the vehicle is fitted with a combined brake system only the type-1 test is necessary.

Every vehicle category has different requirements on average mean deceleration and/or stopping distance depending on what type of brake or brake system that shall be tested. For an L2e-category vehicle with a separate brake system the performance is measured on each axle seperatly for the laden vehicle according to the test conditions prescribed for a type-1 test. The proceedings of a type-1 test are described in table 2.1.3.

Table 2.1.3: Type-1 test proceedings for European L2e-category

Step	Test	Initial speed, v [km/h]	Description
1	Type-0	40	One single stop, stopping distance is noted as S_1
2	-	31.5	A series of 10 repeated stops are performed, after each stop a distance of 1000 meters is driven before next stop
3	Type-0	40	One single stop, performed within a minute after the completion of step 2, the stopping distance is noted as S_2

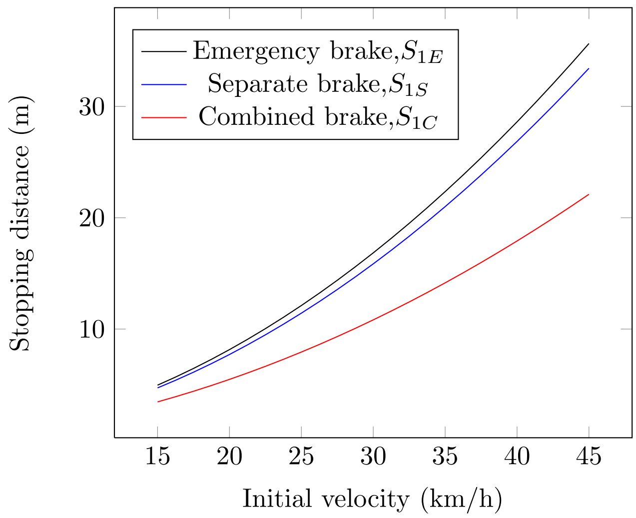

Figure 2.1.1: Legal requirements on combined, separate and emergency brake

The required brake performance on either axle of a L2e-category vehicle are equal and corresponds to, if expressed as deceleration, an average deceleration of 2.7 m/s^2. If it is expressed as stopping distance,the stopping distance must be in accordance with equation 2.1.2. For a combined system the requirements are, if expressed as deceleration, an average deceleration of 4.4 m/s^2. The stopping distance must be in accordance with equation 2.1.3. If an emergency brake exists, this must be able to decelerate the vehicle with an average deceleration of 2.5 m/s^2. Or if expressed as stopping distance, in accordance with equation 2.1.4. Note that an emergency brake is only required on a vehicle with a combined brake system. Figure 2.1.1 show how the stopping distance increases according to equations 2.1.2 thru 2.1.4.

$$S_{1S} \leq 0.1v_1 + \frac{v_1^2}{70} \tag{2.1.2}$$

$$S_{1C} \leq 0.1v_1 + \frac{v_1^2}{115} \tag{2.1.3}$$

$$S_{1E} \leq 0.1v_1 + \frac{v_1^2}{65} \tag{2.1.4}$$

$$S_2 \leq 1.67S_1 - 0.067v_1 \tag{2.1.5}$$

Step 3 described in table 2.1.3 is testing the brake systems residual performance. This residual performance must not be, if expressed as deceleration, less then 60 % of the deceleration figure achived during the first type-0 test. If it is expressed as stopping distance, the stopping distance S_2 must be in accordance with equation

2.1.5, where v_1 is the initial speed. During all of these tests the control force must be recorded and not exceed 200 N for a hand control or 350 N for a foot control. In the case of handbrake levers, the point of application of the control force is assumed to be 50 mm from the outer end of the lever. The parking brake device must, even if it is combined with one of the other braking devices, be capable of holding the laden vehicle stationary on an 18 % up or down gradient. The force applied to the parking brake control must not exceed 400 N, if hand control, or 500 N, if foot control.

2.2 Handling

Handling describes how the vehicle accelerates, decelerates and corners depending on vehicle loads and velocities. Since the vehicle is very light the COG position is affected by the weight and position of the driver and the passengers. The worst case is when a light driver is accompanied by a single heavy passenger since this displaces the COG laterally. For normal vehicles this makes little difference but because of the vehicle properties this factor can affect the handling considerably. The amount of deceleration and lateral acceleration that can be utilized depends on the mass of the vehicle and the COG position. The most critical case to consider is the combination of longitudinal and lateral accelerations that occurs when braking while cornering with the previously mentioned asymmetrical load, see figure 2.2.1.

The vehicle rolls over about the line q between the contact patches of the front and the outer rear wheel as shown in figure 2.2.1. A torque equilibrium about this line is stated in equation 2.2.1. The forces affecting the vehicle is the lateral acceleration due to cornering, the longitudinal deceleration due to braking and the gravitational force which counteracts the first two. The position of the COG, which decides the leverages, is affected by the loading of the vehicle, δy_l, but also by the load transfer caused by the lateral acceleration, δy_{lt}.

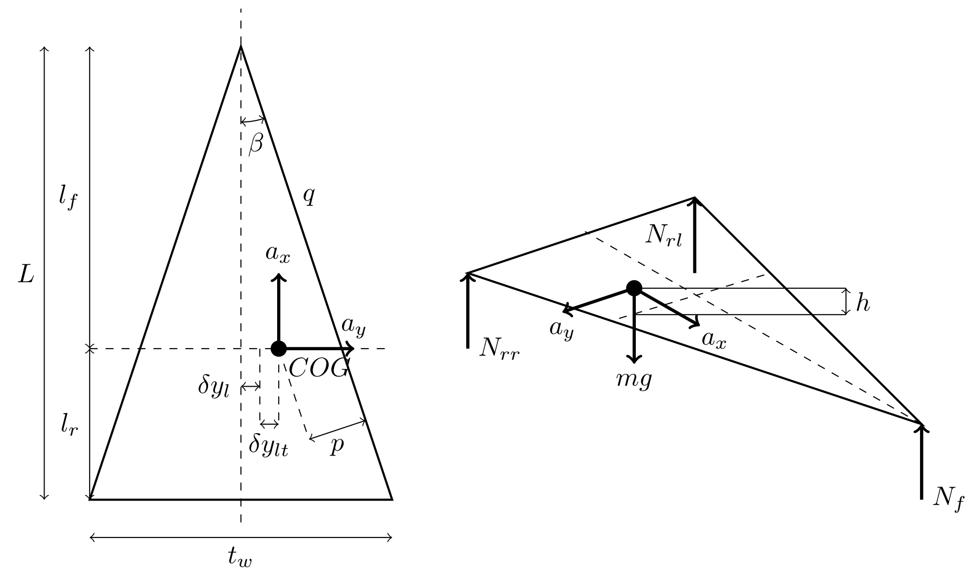

Figure 2.2.1: Handling model, with asymmetrical COG

$$\sum M_q = mgp - ma_x \sin(\beta)h - ma_y \cos(\beta)h \tag{2.2.1}$$

The distance p is determined by adding the lateral COG displacement caused by the vehicle loading to the displacement caused by load transfer. The load transfer is dependant on the roll stiffness which is calculated using equation 2.2.2[**VD**] where K_s is the spring stiffness translated to N/mm wheel travel. The roll stiffness is then used to calculate the roll angle according to equation 2.2.3 where h is the distance from the roll center to the COG which in this case is the same as the COG height above ground. With the chosen types of possible suspension setups the roll axis is situated at ground level.

$$K_\phi = \frac{K_s t_w^2}{2} \tag{2.2.2}$$

$$\phi = \frac{ma_y h}{K_\phi - mgh} \tag{2.2.3}$$

The distance δy_{lt} from figure 2.2.1 is then calculated by using equation 2.2.4. Finally, the distance p can be calculated using equation 2.2.5.

$$\delta y_{lt} = h\tan(\phi) \tag{2.2.4}$$

$$p = l_f \sin(\beta) - \cos(\beta)(\delta y_{lt} + \delta y_l) \tag{2.2.5}$$

By determining these distances the limits of a_x and a_y can be calculated using equation 2.2.1.

2.3 Brake system - general

The braking system is designed with reference to both the requirements of the vehicle and the intrinsic imperatives of the system itself. In the case of vehicle-oriented design, the vehicle's center of gravity and the specified distribution of the braking force to the front and rear axles determine the amount of braking force which can be applied before the wheels lock at any specific coefficient of friction between tire and road surface [**Bosch**].

The dimensioning and design of the brake system components must be able to generate enough brake torque to stop the vehicle with respect to the legal requirements, see section 2.1, given a maximum control force. This control force is usually the force applied by a drivers foot on the brakepedal, in a car etc, or drivers hand squeezing a brakehandle, on a motorcycle etc. The control force can be seen as a boundary condition that determines the design of the braking system. The weight of the vehicle sets the other boundary condition. For any given deceleration, if the weight of the vehicle is increased the braking system must amplify the control force in order to generate adequate brake torque. For this reason, passenger cars and heavy trucks use some sort of power assistance. Most vehicles are also equipped with some type of anti-lock braking system, (ABS), to optimize the usage of the available traction. The available traction is a function of the road friction coefficient and the load on each wheel. Since most vehicles are symmetrical with a lateral COG position on, or very close to, the vehicles centerline, it is for most purposes adequate to use a simplified model as in figure 2.3.1. This model shows the load on the front and rear axles, and the brake force is then assumed to be equally distributed between the wheels on the axle. By applying equations 2.3.1 thru 2.3.3 on the vehicle model in figure 2.3.1 the loads on both axles can be calculated as equation 2.3.4 and 2.3.5.

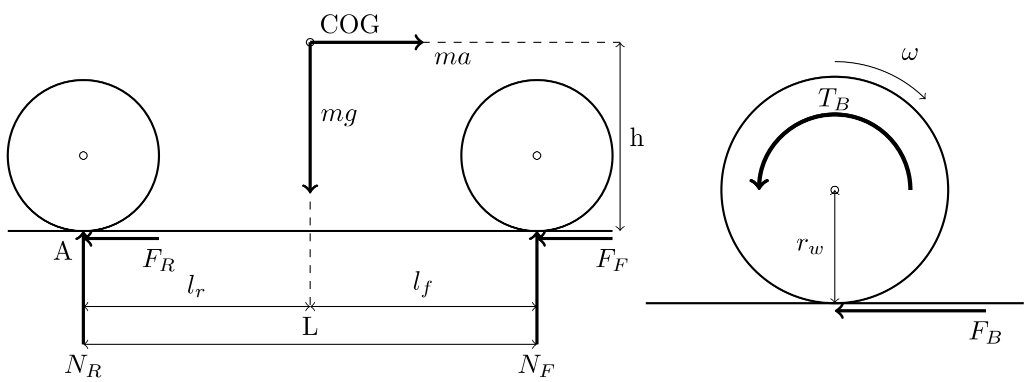

Figure 2.3.1: Braking, simplified models

When the available traction on both axles has been determined a brake system capable of generating enough brake torque to counteract the traction forces can be designed. Figure 2.3.1 show a simplified model for determining the required brake torque which is calculated with equations 2.3.1 thru 2.3.8. Note that the plus-minus sign indicates wheater the vehicle is traveling at an up- or down-hill gradient.

$$\sum F_x = ma - F_F - F_R \pm mgsin\alpha = 0 \tag{2.3.1}$$

$$\sum F_z = N_F + N_R - mgcos\alpha = 0 \tag{2.3.2}$$

$$\sum M_A = mah + mgl_r cos\alpha \pm mghsin\alpha - N_F L = 0 \tag{2.3.3}$$

Since brake tests are performed at zero inclination, the normal forces are:

$$N_R = \frac{m(gl_f - ah)}{L} \tag{2.3.4}$$

$$N_F = \frac{m(gl_r + ah)}{L} \tag{2.3.5}$$

$$F_B = N_{F,R}\mu_{road} \tag{2.3.6}$$

$$\sum T = F_B r_w - T_B = 0 \tag{2.3.7}$$

$$T_B = F_B r_w \tag{2.3.8}$$

The parking brake needs to be able to hold the vehicle at an 18% inclination in any direction for the laden vehicle. It is therefore important to investigate the required road friction coefficient on each axle. If the required friction coefficient is to high at any wheel in a certain direction the vehicle might need to have the parking brake on the other, or on both, axles.

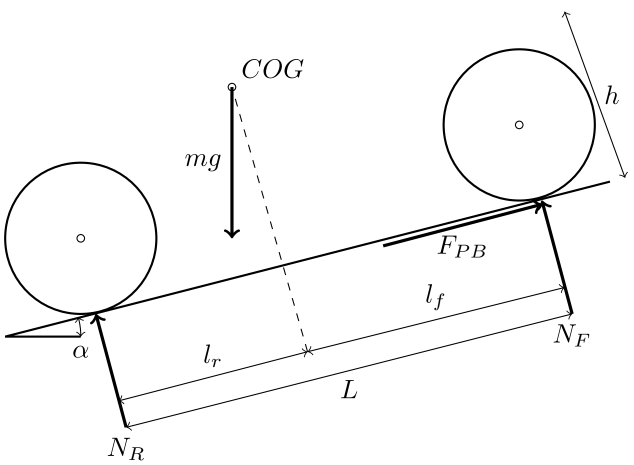

Figure 2.3.2: Required friction coefficient for parking

By examining figure 2.3.2 and using equations 2.3.1 thru 2.3.3, the required road friction coefficient can be determined using equation 2.3.9.

$$\mu_{rec} = \frac{F_{PB}}{N_{F,R}} \tag{2.3.9}$$

Another factor that needs to be considered when deciding where to apply the parking brake is the risk of theft and vandalism. Assuming that the parking brake applies to the front wheel only, since the vehicle is so light, it would be no problem for one person to lift the front end and simply walk away with the vehicle. If it applies to the rear wheels instead it would take two persons to lift the vehicle and one more for steering it. This problem can be solved by chaining the vehicle to a solid object like a lamppost but there will most likely be situations when this is not possible and then its about creating obstacles for miscreants and thieves. The parking brake should preferably be lockable since the vehicle is open.

2.3.1 Brake system setup

There are a number of possible brake system setups to evaluate for the L2e category of vehicles with regards to the definitions on page 3. The added feature of a fully electric L2e vehicle, in contrast to one with a combustion engine, is that the electric motors also can be used to slow down the vehicle and regenerate energy. The different possible hydraulic, mechanical and electrical brake systems are described and discussed in subsections 2.3.2 and 2.3.3. This subsection describes the different possible setups for the CM EULV that are available and allowed with regards to legal requirements and other design criteria. In other words, no components are suggested. The possible setups are shown in figures 2.3.3 thru 2.3.6.

Figure 2.3.3 shows the setup for a combined brake system with a parking brake which also serves as an emergency-brake. This setup is advantageous for the driver, since he/she only has to operate one servicebrake-control in order to stop the vehicle. However, considering that the distribution of the brake torque between the axles might need to be determined by other control systems, due to load changes, in order to ensure acceptable brake performance this might be unacceptable. The parking brake is independent and may act on either, or on both, the front and rear wheels.

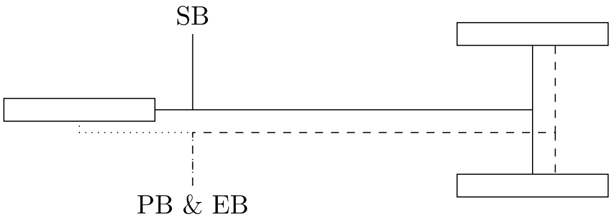

Figure 2.3.3: Combined brake system with parking brake as emergency brake

Figure 2.3.4 shows the setup for a combined brake system with independent parking- and emergency brakes. This system has a great potential for tailoring the different systems to suit their individual purposes. The service brake still suffers from the same problems as described for the previous setup, but a larger issue is that since the brake systems are independent they require a relatively large amount of, or complex, components. The addition of components also increases packaging complexity,weight and overall cost.

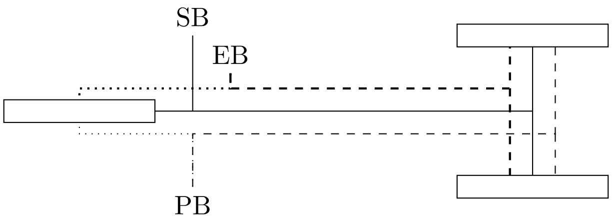

Figure 2.3.4: Combined brake system with independent parking brake and emergency brake

Figure 2.3.5 shows the setup for a separate brake system where one, or both, of the service brakes also works as a parking brake. The separate service brakes allows the driver to control the distribution of the braketorque without adding any other systems. This setup is simple and solves some of the problems that occurs with the combined brake system. The main problem is that, due to the legal requirements regarding the parking brake, see page 3, at least one of the service brakes needs to be purely mechanical.

Figure 2.3.5: Separate brake system with service brake combined with parking brake

Figure 2.3.6 shows the setup for a separate brake system with an independant parking brake. This setup allows the service brakes to be of any type while keeping the parking brake purely mechanical. This setup has the same advantages as the one described with figure 2.3.5 without limiting the options of service brake system layouts. It is however more complex than the previously mentioned setup, because of the separate parking brake.

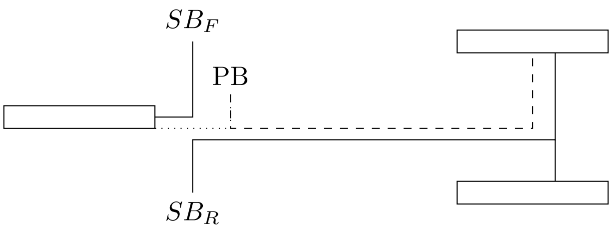

Figure 2.3.6: Separate brake system with an independent parkingbrake

The setups described in figures 2.3.3 thru 2.3.6 all have their different advantages and disadvantages. A combined brake system with a sufficient amount of control systems, such as ABS, is from the perspective of brake performance the best solution. It is the easiest system to handle for the driver and it will regardless the circumstances ensure good brake performance. It is however, for the same reason, one of the most complex solutions which makes it bad with regards to cost and packaging. The alternative to develop a combined brake system without using any active control systems to control the distribution and proportioning of the brake torque exists. The distribution would then be fixed and the brake force would be determined solely by the control force and the dimensions of the components but since the distribution is fixed the brake system can only be optimized for one loadcase. In other loadcases this distribution might limit the maximum brake performance. The braking system using separate brakes for front and rear has the advantage of simplicity, but it requires more experience of the driver in order to achive good brake performance.

2.3.2 Hydraulic and mechanical brake systems

The two types of possible wheel brakes that are applicable to this vehicle are drum- or disc-brakes. There are large variations in design and layout of these brakes. Both can be hydraulic and/or mechanically operated and can, correctly dimensioned, offer enough brake torque to stop the CM EULV. This means that the deciding factor will probably be something other than brake performance. They do however have their different advantages and disadvantages which will make them more or less suitable for the prototype vehicle and the problem is defining the overall best system. Since the CM EULV is propelled by two hub-motors the drum-brake is only an option for the front wheel.

In order to determine what type of brake to use on the front wheel a comparison needs to be made between the brake torque capacity of a drum-brake and a disc-brake. The brake torque for the hydraulic setup, T_{bh}, can be caluculated from equation 2.3.11. Since the parking brake needs to be a purely mechanical brake it is also interesting to investigate the torque capacity of a mechanical disc-brake setup, as this could then also be used as a service brake.

$$r_{bd} = \frac{d_o - d_i}{4} \tag{2.3.10}$$

$$T_{bh} = \frac{F_h L_{hb} A_p \mu_{bd} r_{bd}}{L_{hmc} A_{mc}} \tag{2.3.11}$$

Where:

d_o	=	outer diameter of the brake disc
d_i	=	inner diameter of the brake disc
r_{bd}	=	average radius of brake disc
μ_{bd}	=	friction coefficient between brake disc and brake pad
A_p	=	total area of caliper pistons
A_{mc}	=	area of master cylinder piston
F_h	=	control force, see section 2.1 page 6
L_{hb}	=	distance from handbrake pivot point to point where the control force is applied, see section 2.1 page 6
L_{hmc}	=	distance from hand brake pivot point to point where the force is applied to the master cylinder, depends on the geometry of the brake handle

Equation 2.3.11 assumes a rigid system, i.e. expansion of brake lines and calipers due to pressure and temperature is neglected. Since the vehicle speeds and control forces are low and the brake disc and caliper are not enclosed it is safe to assume that this is a acceptable model.

There are two main types of mechanical floating brake calipers and the difference is in the way they apply force to the brake pad. One uses the actuation of a screw to close the distance between the brake pads and disc and the other uses a simple lever. These types of calipers are used on utility vehicles and ATVs and it should therefore be possible to find suitable standard components. Since the setup is similar to that of a hydraulic brake system calculating the brake torque will also be similar. The difference will be in the transfer between the brake handle and the brake pad. If mechanical calipers of appropriate dimensions are found the brake torque must be calculated according to their intrinsic properties.

There are a large number of different designs of drum brakes, but they all consists of the following main parts: leading and trailing shoes (in free combinations), linings, a brake drum and an activation mechansim [**Drumbrake**]. Since there are so many different combinations and types of shoes and activation mechanisms it is very difficult to give a general discription of how to calculate the brake torque capacity. The easiest way to analyse drum brakes is to assume elastic linings and stiff brake drum and brake shoes. It is assumed that the contact geometry of the drum and lining is independent of the brake shoe actuating force or motion. Consequently, the pressure on a small lining is reduced to a simple trigonometric shape [**Drumbrake**]. This method is however insufficient since small variations in either parts can have large impacts on the brake performance. In 1973 Millner [**Millner**] presented an elastic concept. This concept includes an elastic shoe and drum model.The shoe was modelled as a curved elastic beam subjected to radial and frictional load. Moreover, the lining was divided into a number of elements. The drum was modelled as a thin ring loaded only in the radial direction. The tangential (frictional) force is not accepted by the model. The pressure distribution is calculated using the concept of influence coefficients, which are determined empirically and used as input data in a computer program[**Drumbrake**].

Since the required brake torques will be relatively small, it is for this thesis sufficient to use the rigid model as an approach to evaluate what drum brakes are suitable or not. The type of drumbrake that will be examined is a drumbrake with a single internal expanding shoe as described by Mägi and Melkersson [**Magi**],see figure 2.3.7. With a known pressure distribution the braketorque can be calculated from equation 2.3.12.

$$T_{bd} = \int_{\phi_1}^{\phi_2} \mu p(\phi) b R^2 \, d\phi \tag{2.3.12}$$

Using the pressure distribution hypothesis based on wear, the wear is described as;

$$w = \frac{pR\omega}{W} \tag{2.3.13}$$

Where W is the wear resistance. The wear-rate on the brake-pad at angle ϕ is;

$$w = \dot{\Theta} A \sin\phi \tag{2.3.14}$$

Combine equations 2.3.13 and 2.3.14 to get the pressure distribution;

$$p(\phi) = p_{max} \sin\phi \tag{2.3.15}$$

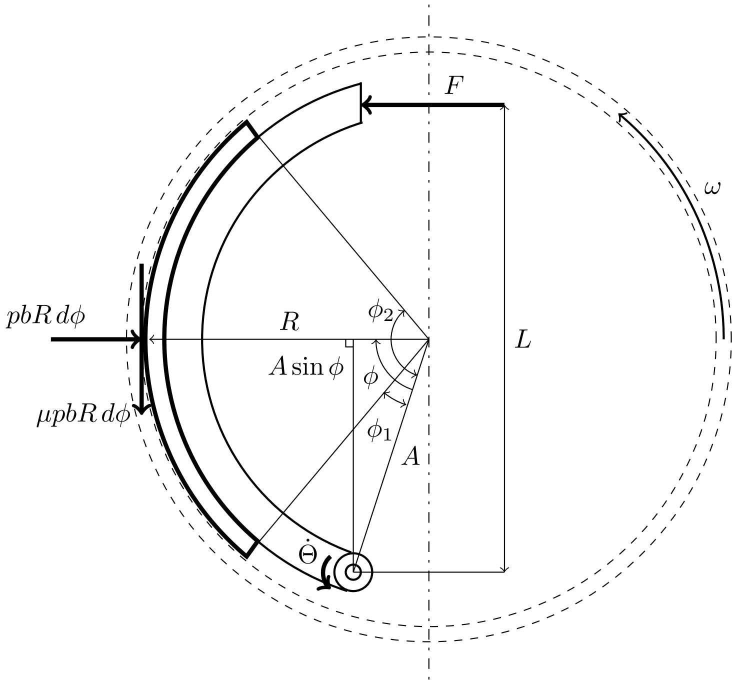

Figure 2.3.7: Geometry and forces in a single shoe drum brake

Torque equilibrium around the shoes pivot point results in;

$$FL = \int_{\phi_1}^{\phi_2} p(\phi) bR\,d\phi A\sin\phi - \int_{\phi_1}^{\phi_2} \mu p(\phi) bR\,d\phi (R - A\cos\phi) \tag{2.3.16}$$

Where b is the width of the drum. By combining equation 2.3.15 and 2.3.16 the integrands before integration can be systematically divided into often reoccuring integrals for brake analysis with explicit solutions;

$$I_s = \int_{\phi_1}^{\phi_2} \sin\phi\,d\phi = \cos\phi_1 - \cos\phi_2 \tag{2.3.17}$$

$$I_{ss} = \int_{\phi_1}^{\phi_2} \sin^2\phi\,d\phi = \frac{\phi_2 - \phi_1}{2} - \frac{\sin 2\phi_2 - \sin 2\phi_1}{4} \tag{2.3.18}$$

$$I_{sc} = \int_{\phi_1}^{\phi_2} \sin\phi\cos\phi\,d\phi = \frac{\cos 2\phi_1 - \cos 2\phi_2}{4} \tag{2.3.19}$$

Equation 2.3.16 can then be written as;

$$F = \frac{p_{max} bR^2}{L}\left[\frac{A}{R} I_{ss} - \mu\left(I_s - \frac{A}{R} I_{sc}\right)\right] \tag{2.3.20}$$

According to equation 2.3.12 the brake torque is;

$$T_{bd} = \mu p_{max} bR^2 I_s \tag{2.3.21}$$

By eliminating p_{max} from equation 2.3.20 and inserting it in equation 2.3.22, a relation between brake torque T_{bd} and force F is found.

$$T_{bd} = \frac{\mu I_s}{\frac{A}{R} I_{ss} - \mu\left(I_s - \frac{A}{R} I_{sc}\right)} FL \tag{2.3.22}$$

Note that the force F is not the control force. Depending on the design of the drum brake the control force will be transferred either by hydraulics or mechanical links. For simplicity the brake torque will be considered as doubled if a two-shoe drum brake is used.

For all the brake systems mentioned in this section the force generated at the tire contact patch is determined by equation 2.3.8, which is the force that needs to be compared to the available traction.

To get a general idea what stopping distance that can be expected from different hydraulic or mechanical brake systems Newtons laws of motion are used. By establishing the brake force that can be generated for a specific brake system, for the maximum allowed control force, a brake force and accelerations vector can be determined, see equation 2.3.23. It is important to check and see if the maximum generated brake force exceeds the available traction, if so this implies that the wheel has locked up and the system needs to be reviewed. Since the application of the control force is not a step function the brake force is assumed to reach its maximum value after a short period of time, see Appendix B.

$$a(t) = \frac{F_B(t)}{m} \tag{2.3.23}$$

The acceleration vector is used to determine the velocity according to equation 2.3.24 and the stopping distance can be calculated using equation 2.3.25.

$$v(t) = v_0 - a(t)t \tag{2.3.24}$$

$$S = \int_{t_1}^{t_2} v(t)\, dt \tag{2.3.25}$$

2.3.3 Electrical brake system

Since the vehicle is going to be propelled by two hub motors, there are good reasons to look into some form of electrical braking. The hub motors can be used as generators and thereby regenerate some of the kinetic energy. Ideally this energy could be used to recharge the battery. This is possible since the converter is a 4-quadrant converter capable of handling both positve and negative currents. The other option is to let the energy go to waste in a resistance. Depending on the sensitivity of the motor controller electronics and the maximum output of the motors, a system could be devised to assist a hydraulic or mechanical brake system, or ideally be sufficient for braking on its own.

In order to determine if the existing hub-motors could brake the EULV in accordance with the legal requirements the power demand must be calculated. An easy way to get a general idea of the power necessary to brake the vehicle is to consider the kinetic energy of the EULV at a given speed, and then subtract an amount of energy every time step and from that determine an estimated stopping distance. The kinetic energy of a non-rotating object is determined by equation 2.3.26.

$$E_k = \frac{mv^2}{2} \tag{2.3.26}$$

By converting a constant amount of energy, either regenerate or convert to heat, over a period of time the performed work is;

$$W = \Delta E_k = E_{k1} - E_{k2} = \frac{m}{2}(v_1^2 - v_2^2) \tag{2.3.27}$$

Since there is no generally accepted method to simulate the braking behaviour for EULVs, and the goal is to get an estimate rather than an exact value, a constant rate at which energy is converted is assumed. For constant power P, the amount of work done, or energy converted, during a period of time T is given by equation 2.3.28. According to CM the maximum input for this type of motor is approximatley 2.5 kW per motor. This is therefore the upper limit of energy conversion.

$$W = PT \tag{2.3.28}$$

This means that the power demand can be determined granted that an assumption is made on how long it should take to stop the vehicle. With the time-assumption it is also possible to determine the stopping distance.

Since the velocity at any point is a function of the remaining kinetic energy, the stopping distance is determined by integrating the generated velocity-time function.

$$v_k = \sqrt{\frac{2\Delta E_k}{m}} \tag{2.3.29}$$

$$S = \int_{t_1}^{t_2} v_k(t)\,dt \tag{2.3.30}$$

This analysis does not determine the braking force at the tire contact patch, since there is no risk of the rear wheel locking up. If a to high current is is requested compared to the available traciton the wheel will lock momentarily, which means no current will be produced and the wheel will start rolling again. There are a number of other intrinsic problems with using generators as brakes that needs to be adressed. Due to the low resolution of the motor, the standard control unit can not handle low power inputs. If better control units are installed the current can be reversed at low rotational speeds and effectively try to reverse the vehicle. Another problem is that in order to be able to use generator brakes effectively, the driver should be able to adjust the power input, which requires an extra control system. There are a number of possible ways to implement generator brakes. One option is to only use them during coasting i.e. at any time no throttle is applied. Another one is to have the generator brake controlled by one of the brake controls, for example connected to the existing brake light switch. This setup could enable a constant amount of braking power to be applied at the same time as the brake light switch is engaged. If the amount of power is to be proportional to the brake force generated by the hydraulic or mechanical brake system connected to the brake control, a control system needs to be designed.

2.4 Brakes - summary

There are a number of factors to to take into account when deciding what type of brake system and components that should be used for any type of vehicle. In many cases there are only a few acceptable options with regards to legal requirements, cost and packaging etc. However for this type of vehicle there are a large number of options since the requirements are relatively few and the demands are low. Supposing that a combination of the previously mentioned hydraulic and mechanical brake systems could fulfill the legal requirements, the next step is to determine which setup that should be used. The choice of setup is more a question of cost and packaging. A more complex setup will require more components and control systems, while a simple setup will need less components and uses the driver as a control system. The main issue regarding the brake system setup is how to incorporate the parking brake without adding an entire system. Since the parking brake needs to be purely mechanical this could determine that one of the service brakes needs to have a purely mechanical transmisson. Because of the size and design of the vehicle a natural choice of components are those applicable to mopeds, motorcycles and utility vehicles. The options are to either use a drum brake with mechanical, or combined, transmisson for the front wheel or mechanical, or combined, brake calipers for the rear wheels. The problem is that combined brake calipers are not common among these types of vehicles and it will therefore be difficult to find appropriate standard components.

2.5 Suspension - general

The suspension setup is not constrained by any legal requirements. The design is nonetheless very important for the vehicle in many regards. With the CM EULV the most important factors are cost, packaging and weight. One of the goals of the thesis is to evaluate two different concepts for a rear suspension setup which makes the vehicle safe to handle and also provides a comfortable ride. In addition, both concepts must be adapted to the chassis when it comes to loadpaths and packaging. It is desirable to keep the space between the rear wheels clear in order to fit a luggage compartment. This suggests a swing type suspension which builds forwards instead of inwards. Since the vehicle is a three wheeler the rear track width should be maximized without exceeding the specified vehicle width. The composite body also has limitations regarding how forces can be applied. Distributed loads are desirable while point loads and shear forces requires additional attention. It is also desirable to concentrate the forces to the rear end of the bottom plate of the body since this will be the split line between the bottom and the rear end of the body. This means that this section will be very strong and capable of handling large forces.

The rubber suspension axle that was mounted on P1A at the beginning of the thesis became one of the alternatives. Benchmarking of existing three wheelers as well as mopeds and motorcycles led to the second one which utilises swing arms with shock absorbers similar to many motorcycles.

Regardless of the type of suspension setup chosen, a major concern exists regarding the roll behaviour of the vehicle. This is especially important since the vehicle is a three wheeler with a single front wheel. This kind of vehicle exhibits a risk of rollover during for example evasive manouvers or when braking while cornerning. Reducing the vehicle's tendency to roll reduces this risk while at the same time increasing the driver's confidence in the vehicle. This reduction can either be accomplished by increasing the suspension stiffness or by implementing an anti roll bar. The anti roll bar is the preferred option since it allows the suspension springs to be relatively soft which ensures better comfort. The negative part is that it adds complexity, cost and weight.

2.5.1 Shock absorber suspension setup

The spring and damper solution is a widely used concept. It is in some form utilised in most passenger vehicles currently produced. Beacuse of the wide usage there is also a great supply of components at virtually every level of cost and size. This means it should be possible to purchase a suitable setup, at a fair price, without having to develop anything from scratch.

The main concern regarding this setup is the packaging, see figure 2.5.1. In order for the shock absorbers to have enough stroke, the damper must be of a certain length. The relationship between the damper stroke length, vertical wheel travel and the transferred forces are dependent on the shock absorbers mounting points. Consider the swingarm axle as fix. A mounting closer to the wheel decreases the amplificiation of the normal force on the rear wheel, while the vertical wheel travel approches the damper stroke length. A damper mounted closer to the chassis increases the vertical wheel travel which means that there will be a tradeoff between acceptable forces for the chassi and percieved comfort. The angle of the damper also affects the magnitude and direction of the forces. The optimum would be to position the damper perpendicular to the swingarm for straight loadpaths but because of the very limited space this is not possible. There is also a decreasing amount of mounting space as the mounting points move forward due to the slope of the rear seats.

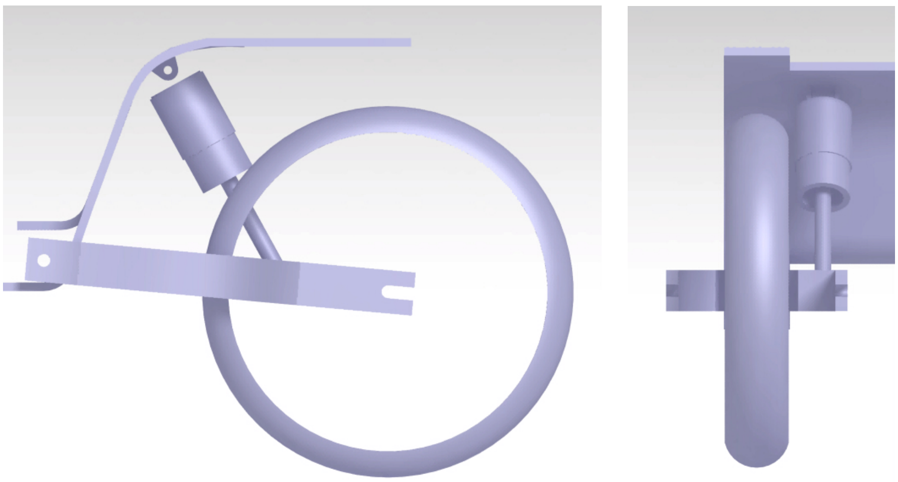

Figure 2.5.1: Placement of shock absorber on CM EULV

The mounting to the chassis is also an issue since the composite body only can deal with forces of certain types and magnitudes. The point load induced by the upper damper mounting must be handled with some kind of insert which adds weight and complexity to the body. The size and direction of the force decides the size of the insert. This means it is desirable to keep the force small and also perpendicular to the surface since the sandwich construction is bad at handling shear forces. The mounting between the swing arm and body also requires some kind of insert but the bottom part of the body is stronger which means these forces should be easier to deal with.

For the shock absorber setup a suitable spring stiffness needs to be determined. Softer springs makes the ride smoother at the cost of a vehicle that rolls more and so becomes more difficult to drive. With too soft springs there is also a risk of hitting the bumpstop of the damper. If this happens during regular driving it will make the ride jerky and the suspension components might be damaged. Too stiff springs can also cause jerky suspension behaviour since a large part of the forcepeak caused by a bumb will be transmitted to the chassis causing an uncomfortable ride. One possibility to solve this problem might be to use springs with progressive stiffness. These are soft at small deformations, helping to provide a comfortable ride, while the stiffness increases at large deformations to improve the vehicle dynamics.

2.5.2 Rubber suspension axle setup

The rubber suspension axle is an old suspension solution which has been used on cars in the past. The version using rubber as spring and damper is currently mostly used on trailers and caravans as well as in some agricultural appliances. One version of this is based on two different sized square steel pipes. The bigger is mounted to the chassis of the vehicle. The smaller pipe is pressed into the bigger one with four rubber rods between them as shown in figure 2.5.2. The swing arm with the wheel is then mounted to the smaller pipe and when the wheel moves up and down the rotation between the two pipes causes the rubber to deform. The viscoelastic properties of the rubber material makes it act as both spring and damper.

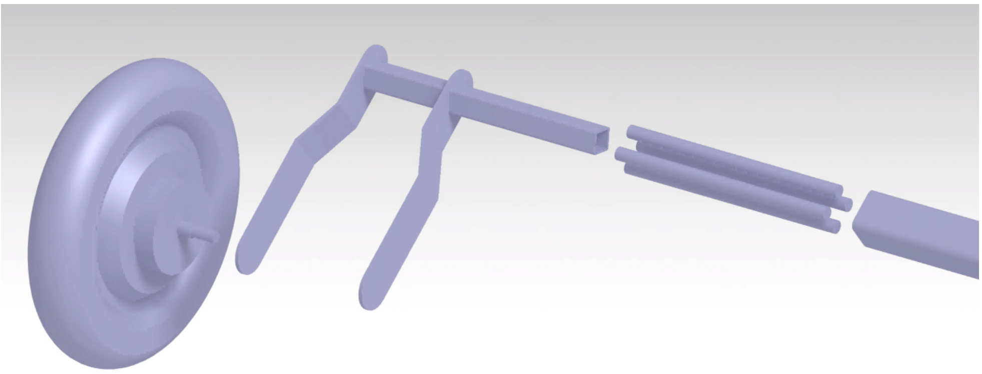

Figure 2.5.2: Exploded view of rubber suspension axle

The standard version of this concept utilizes a longer outer pipe which spans the width between the tires of the vehicle. One small pipe is then pressed in from each side to accomodate the swing arms and wheels as shown in figure 2.5.3. This induces bending moments into the axle since the wheels are mounted outside of the rubber rods. Another version of this concept is to make two individual suspension sections, one for each wheel. The wheel could then be mounted as shown to the right in figure 2.5.4. This concept eliminates the bending moments induced by the mounting shown to the left in figure 2.5.4. The possible advantages for the split design is reduced weight and easier handling of the suspension sections when assembling the vehicle. The disadvantage is that the axle, and the rubber rods, needs to be made shorter, preferably no wider than the wheel in order to be able to use straight swing arms. This means that thicker, stiffer, rubber rods needs to be used and the cross section of the axle becomes larger.

The mounting of these suspensions suits the design of the body since all the forces and moments are transmitted through the larger pipe section into the body. This pipe could be positioned in the split-line between the two body parts which should make the mounting easy. Another advantage with this force-path is that all the vibrations coming from the wheels and motors must travel through the rubber before they can get into the passenger compartment. The rubber therefore helps to cancel out much of the noise and vibrations that would otherwise be a disturbance to the driver and passengers.

The rubber suspension axle fits the general vehicle design well since it is probably possible to integrate the outer pipe into the body structure which makes for a very clean design where the only visible parts of the suspension is the swing arms. The main property of the trailer axles that must be optimized in order to fit the CM EULV concept is the weight since this is less important for trailers which focus more on robustness. Since the entire construction consists of steel pipes considerable weight could be saved if the material could be

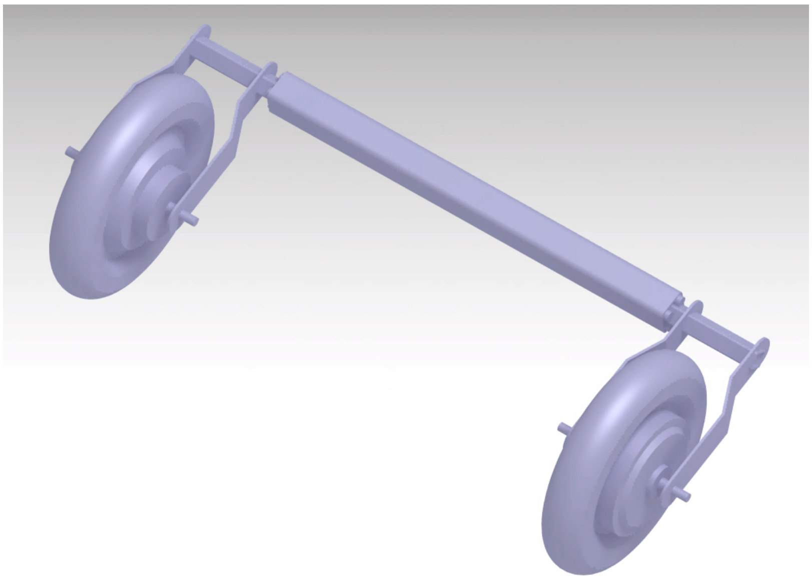

Figure 2.5.3: Assembled view of rubber suspension axle for CM EULV

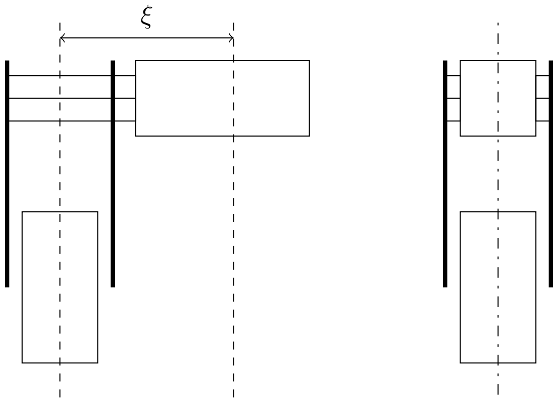

Figure 2.5.4: Different mounting options for rubber suspension axle

replaced by a lighter alternative.

2.5.3 Anti-roll bar

The roll behaviour of a three wheeled vehicle is especially important since there is a risk that the vehicle might roll over if handled incorrectly. This behavior can be counteracted by increasing the stiffness of the suspension, however this also leads to a decrease in comfort. The tendency to roll can be reduced, without affecting the suspension stiffness during bump, by implementing an anti roll bar. This solution has no effect when the vehicle hits a bump and both wheels move together. When the vehicle rolls, i.e when one wheel moves up and the other moves down, the anti roll bar counteracts this motion by applying a moment in the opposite direction proportional in size to the roll angle. This also means that during bump with one wheel, for example on an uneven road, the anti-roll bar will have a negative influence on the suspension.

The concept for implementing an anti-roll bar on the CM EULV is to mount a spring bar or pipe between the swing arms in their axis of rotation. When the rotations of the swing arms differ, i.e. when the vehicle rolls, the anti-roll bar will twist and cause a moment that tries to decrease this difference.

The torsion constant of an anti roll bar in the form of a solid circular bar and a circular pipe can be calculated using equation 2.5.1 and 2.5.2 respectively.

$$J = \frac{\pi}{2} r^4 \tag{2.5.1}$$

$$J = \frac{\pi}{2}(r_o^4 - r_i^4) \tag{2.5.2}$$

This value can then be used in equation 2.5.3, where G is the material shear modulus, to calculate the relation between torque and angle of twist in the anti roll bar.

$$T = \frac{\phi JG}{l} \tag{2.5.3}$$

The relation between vehicle roll angle and angle of twist in the anti roll bar is given by equation 2.5.4.

$$\theta = 2\arcsin(\frac{t_w \tan\phi}{2l_{swing}}) \tag{2.5.4}$$

2.6 Suspension - summary

The mentioned suspension setups and components all have positive and negative properties that must be considered when designing the final vehicle concept. The most important factors are cost, packaging and weight. Besides these factors the safety must be considered along with the vehicle handling.

The advantages of the shock absorber solution is that it is very predictable when it comes to vehicle handling. The loadpaths in this setup are theoretically better than in the rubber suspension axle setup since there are two mounting points on each side. The extra mounting points requires additional inserts which makes it less suited for the CM chassis design. This means that weight can be saved on individual suspension components but it also adds weight and cost to the body. The suspension is also split in two separate sides which means the assembling should be easier. The negative sides when compared to the rubber suspension axle is that it has more parts and more complexity. The cost will also be a disadvantage for the shock absorbers. Even if the ideal components are found and can be ordered in large quantities they will never be as cheap as the pipes and rubber rods of the rubber suspension.

The positive aspects of the rubber suspension axle apart from being cheap is that it is very simple. It has few components and there is a potential for making it light. The simplicity also makes it easy to maintain since there are few parts that can break. The ability to reduce the noise coming into the passenger compartment is also better than for the spring/damper solution. The negative side is that the behaviour of the rubber suspension axle is very hard to predict and therefore difficult to optimize.

The anti-roll bar enhances the driveability of the vehicle at the cost of more parts and increased weight and complexity. The amount of increase depends on which suspension setup is used. The shock absorber setup and the split rubber suspension has free space between the swingarm mounting points. This means the anti-roll bar can be made short and with the desired diameter. With the regular rubber suspension the anti-roll bar must run through the entire axle and be attached on both sides. This means that, in comparison, the bar must be longer and thinner. Both of these factors reduces the effect of the anti-roll bar.

3 Method

This chapter describes the various methods and softwares used for analysing and simulating the different parts of the problem definiton.

3.1 Static calculations and CAD

The static calculations were performed using Matlab. These calculations are mainly based on Newton's laws of motion and simple trigonometrics. The CAD software CATIA V5 was used for various purposes. In order to verify dimensions and behaviours of different suspension setups, models where created in CATIA V5 and virtually tested. Figure 6.2.3 in Appendix A shows a working model used to test packaging and vertical wheel travel for a shockabsorber suspension setup. By applying constraints to the swingarm, shockabsorber and wheel, the calculated values of ride height, vertical wheel travel and shock absorber compression could be validated.

3.1.1 SC - Center of gravity

The position of the vehicle's center of gravity, COG, plays an important role for both the performance of the brakes and the handling of the vehicle. In order to properly analyse these systems the location of the COG was determined. The first existing prototype, and CATIA model, was used to get the necessary input data. In the

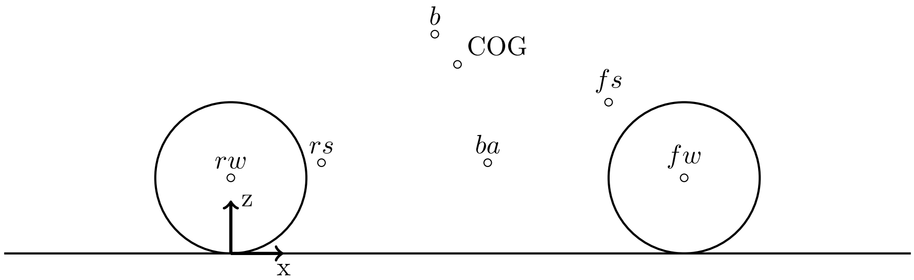

Figure 3.1.1: Location of subsystem COGs

CAD-model the location and weight of each major subsystems COG was determined using CATIA. To get the COG for the whole vehicle a torque equilibrium was calculated around the rear wheel axle, see figure 3.1.1. Solving equations 3.1.1 and 3.1.3 for x_{COG} and z_{COG} respectively gives both the longitudinal and vertical position of the COG.

$$\sum M_{ox} = m_{COG}x_{COG} - (m_{rw}x_{rw} + m_{rs}x_{rs} + m_b x_b + m_{ba}x_{ba} + m_{fs}x_{fs} + m_{fw}x_{fw}) = 0 \tag{3.1.1}$$

$$x_{COG} = \frac{m_{rw}x_{rw} + m_{rs}x_{rs} + m_b x_b + m_{ba}x_{ba} + m_{fs}x_{fs} + m_{fw}x_{fw}}{m_{COG}} \tag{3.1.2}$$

$$\sum M_{oz} = m_{COG}z_{COG} - (m_{rw}z_{rw} + m_{rs}z_{rs} + m_b z_b + m_{ba}z_{ba} + m_{fs}z_{fs} + m_{fw}z_{fw}) = 0 \tag{3.1.3}$$

$$z_{COG} = \frac{m_{rw}z_{rw} + m_{rs}z_{rs} + m_b z_b + m_{ba}z_{ba} + m_{fs}z_{fs} + m_{fw}z_{fw}}{m_{COG}} \tag{3.1.4}$$

Where:

fw	=	front wheel
rw	=	rear wheel
fs	=	front suspension
rs	=	rear suspension
b	=	body
ba	=	battery

The COG position of the target vehicle became an approximation based on both calculations and physical testing. The target vehicle will differ from the prototype both in total weight and the weight distribution. But for the continuation of this thesis, an average COG position needs to be determined. By using the unladen vehicle COG and adding COGs for driver and passengers, the weight transfer as a function of number of occupants can be determined.

3.1.2 SC - Brakes

In order to determine which combination of components that best suit this vehicle, a matrix of possible solutions needs to be created. By using the equations in section 2.3 and 2.3.2 the required brake torque will be determined in accordance with the legal requirements, see 2.1. Then a selection of components must be made with regards to packaging, weight and cost. Subjective opinions and measurements gathered from test drives are also included in order to determine the overall best solution.

3.1.3 SC - Handling

The calculations concerning the handling were performed in order to see the effects of combined braking and cornering during various loads. The equations from section 2.2 were used in Matlab to produce plots showing the effects of asymmetrical vehicle loading. The handling will also be evaluated by test driving the existing prototypes.

3.1.4 SC - Suspension

Calculations regarding the suspension setups were mainly done for dimensioning purposes. The first step was to make models for the geometries that could then be used, together with the loadcases, to calculate the resulting forces. These forces can then be used for designing and weight optimizing the suspension components and the body structure.

The shock absorber solution geometry was set up using constraints from all the different components. It is desirable to make the damper itself as long as possible in order to achieve the wanted characteristics at a low cost. The optimum position of the damper is in line with the tire since this gives straight force paths but because of the limited space between the tire and the chassis it might be necessary to place it at the side of the wheel instead. The angle of the damper should be kept perpendicular to the swing arm in order to minimize the reaction forces in the mounting points. The same is true for the angle between the damper and the chassis but since the chassis is not parallel to the swingarm a compromise might be necessary. A Matlab program was set up taking these factors into consideration. In the program the intervals for possible mounting points and acceptable force levels could be narrowed down to achieve a suitable suspension geometry.

The standard rubber suspension axle has a simpler geometry were the only thing that can be altered is the length of the swing arm. All the forces in this suspension setup goes into the chassis through the larger axle pipe which makes the calculations simple. The split axle design simplifies this even further since the bending moments are minimized. Both cases gives forces and moments that can be used to dimension the chassis and the suspension components.

The effect of utilizing an anti-roll bar was simulated with a Matlab program. The program calculates the vehicle roll angle at a certain lateral acceleration. An anti-roll bar with a specified geometry is then applied according to the equations in section 2.5.3 and the resulting decrease in roll angle is calculated.

3.2 Physical testing

The physical testing was conducted to validate the calculations and because certain simulations were too time consuming or too unreliable.

3.2.1 PT - Center of gravity

The location of the COG of the prototype vehicle was determined by weighing the vehicle at different angles of inclination between the front and rear axle. The load transfer resulting from a change of the angle is caused by the COG height which can then be determined. Figure 3.1.1 shows the principle while the calculations are shown in equations 3.2.1 thru 3.2.5.

Together with the measured values of the normal forces N_f and N_r, equations 3.2.1 and 3.2.2 gives the values of l_r and $l_{r,incline}$ for plane and inclined weighing respectively.

$$N_r l_r = N_f l_f \tag{3.2.1}$$

$$L = l_f + l_r \tag{3.2.2}$$

The values of the parameters a and b represent the difference in l_r caused by the inclination and the height of the COG respectively. These are calculated using equations 3.2.3 and 3.2.4.

$$b = l_f(1 - cos\alpha) \tag{3.2.3}$$

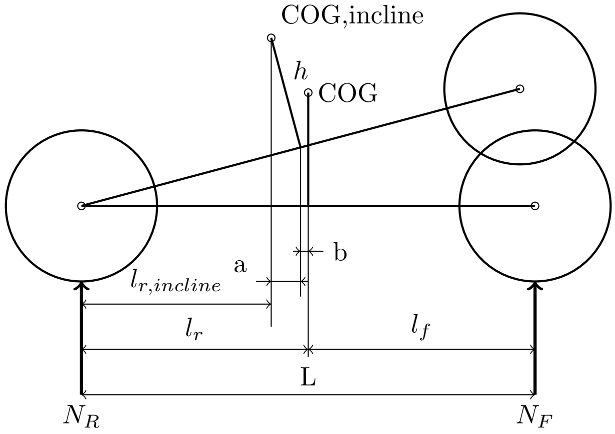

Figure 3.2.1: Determination of prototype COG

$$a = l_r - l_{r,incline} - b \tag{3.2.4}$$

The height of the COG can then be calculated using equation 3.2.5.

$$h = \frac{a}{sin\alpha} \tag{3.2.5}$$

3.2.2 PT - Brakes

The brake testing was performed only by actual driving. The stopping distance was measured from given initial velocities according to section 2.1. The brake setups were also tested to measure the drivers subjective experienced confidence in different components and ways of braking. Measurements of average deceleration have not been attemted due to a lack of equipment.

Since the prototypes all have different brake system setups its important to test them all and compare them on equal terms. The stopping distances were recorded according to the legal requirements for all prototypes inline with their respective systems. Which means that each vehicles brake system have been tested either separatly or combined. Its important to record the total weights of each vehicle during the tests to get more accurate calculations.

3.2.3 PT - Suspension

Both suspension setups were tested subjectively by driving the prototype vehicles through various tests which are shown in figure 3.2.2. The first test is the skidpad, which means driving in a circle for testing cornering capacity. This is done at a certain speed and the result is measured by the radius that the vehicle can handle without lifting the innner wheel or skidding off track. The next test is the evasive manouver, which simulates a suddenly appearing obstacle. This is performed by entering the test area through a corridor and exiting through another, offset from the first one. The final handling test consists of driving slalom between cones. The different setups were also tested for driver and passenger impressions regarding handling and steering during regular driving.

The shockabsorbers on the P1B had a spring pre-tension which was variable in five steps. The pre-tension sets the force required for the initial spring deformation. The vehicle was tested with this setting in different positions. To evaluate the anti-roll bar a simple version was mounted to the rubber suspension axle during one of the test sessions. Subjective testing was performed by regular driving and slalom tests to get impressions from the driver about the handling of the vehicle. Objective testing was carried out on the skidpad by testing the cornering capacity at identical conditions, with and without the anti-roll bar. The spring and damper suspension setup was also disassembled in order to determine the spring stiffness. This was done using a press and a scale as shown in figure 3.2.3.

The press was used to deform the spring and the spring length was measured at different loads in order to acquire a force-deformation diagram. This was then used to simulate the setup with different spring stiffnesses. Stiffer springs were then mounted and evaluated by driving the vehicle.

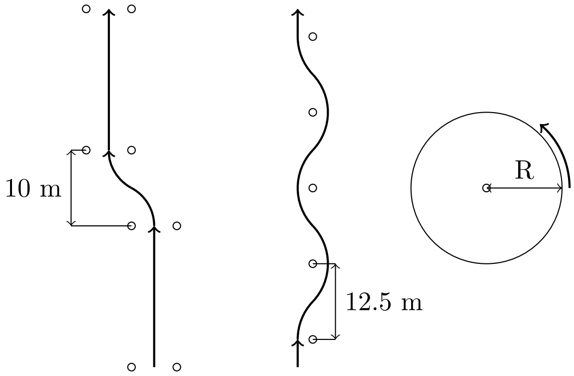

Figure 3.2.2: Evasive maneuver, slalom and skidpad test setup

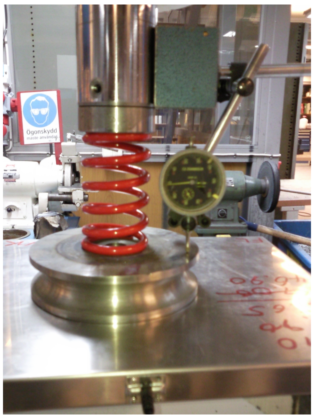

Figure 3.2.3: Testing of spring stiffness

The rubber suspension axle was also tested separately besides the actual driving. The testing was conducted in order to evaluate the effect of making the axle shorter which would be necessary to implement the split axle design introduced in section 2.5.2. This testing was conducted by mounting a section of the suspension axle, with swing arms and wheel axle, to a rigid block as shown in figure 3.2.4.

Figure 3.2.4: Testing of torsion axle

Different loads were then applied at the wheel axle and the deformation was measured. Three series of measurements were performed and then the axle was shortened. This was repeated for two different sizes of axles and four different lengths of each axle.

4 Results

The results section is divided into COG position, brake performance and suspension performance.

4.1 Estimated COG

The COG was calculated in two different ways. The first was by weighing the prototype vehicle and the second was to divide the vehicle in subsystems and adding up the weight and COG for each one based on the CAD material. Three separate weighings were performed with different angles of inclination. The values from these cases were then used together with the equations from section 3.2.1 to calculate the COG position. The results are presented in table 4.1.2.

Table 4.1.1: Determining the COG position on prototype vehicle

	Inclination angle [deg]	Front scale reading [kg]	Rear scales reading [kg]	l_f [m]	h [m]
Weighing 1	0	74.3	87.9	1.06	reference
Weighing 2	-2.75	75.5	87.0	1.05	0.26
Weighing 3	5.5	72.3	90.6	1.08	0.29

The second way of determining the COG was to use the CAD model. The weight and COG postition for each subsystem is presented in table 4.1.2. Equations 3.1.2 and 3.1.4 was then used to determine the COG position for the whole vehicle, which is also presented in table 4.1.2. The results from these two different approaches

Table 4.1.2: Determining the COG position using CAD

	Front wheel	Rear wheel	Front suspension	Rear suspension	Body	Battery	Total
Weight [kg]	5.5	31.2	5.5	26	72	22	161.7
COG to ground [m]	0.2	0.2	0.669	0.246	0.803	0.335	0.414
COG to front axle [m]	0	1.963	0.155	1.619	1.120	0.918	1.270

were then merged into an approximate COG position. This position is presented in table 4.1.3 together with the COG positions for the driver and passengers aswell as the total for the two loadcases previously presented.

Table 4.1.3: Estimated COG position

	Unladen vehicle	Driver	Passengers	Vehicle +driver	Vehicle+driver +passengers
Weight [kg]	162.2	75	2x75	237.2	387.2
COG to ground [m]	0.4	0.842	0.705	0.54	0.6
COG to front axle [m]	1.3	1.049	1.722	1.2	1.4

These values will be used as standards for this thesis when calculating brake- and suspension performance.

4.2 Brake performance

The brake performance was evaluated thru calculations and test drives. Subjective opinions of all testdrivers have been percieved thru the course of the thesis and are also considered.

4.2.1 Brake dimensioning

In order to determine how the brake force needs to be proportioned equations 2.3.4 and 2.3.5 are used. By plotting the normal forces as functions of the deceleration, assuming a road friction coefficient, figure 4.2.1 can be constructed. The blue and red lines represent the front and rear lock up lines for a vehicle weight of 225 kg and 385 kg. The green lines show how the brake force should be proportioned between the front and rear axle. The black dashed lines show constant decelerations of 2.7 m/s^2 and 4.4 m/s^2, which are the requirements for separate and combined brake systems.

For most vehicles with combined brake systems it is preferable to have a proportioning strategy which lets the proportioning line intersect the front lock up line before the front- and rear lock up lines intersect. This is

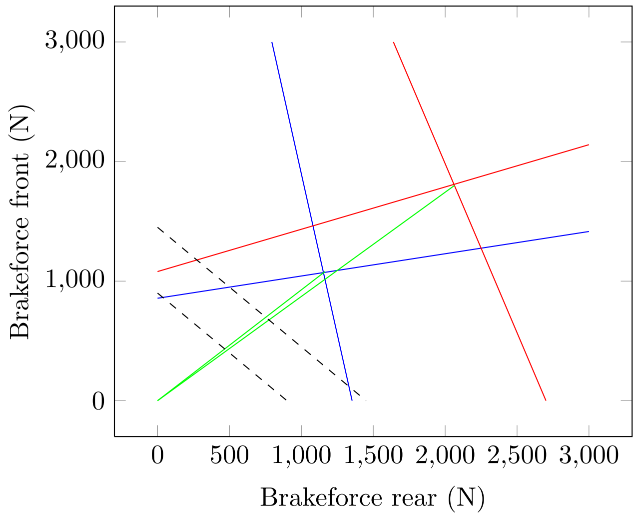

Figure 4.2.1: Brake proportioning for 225 kg and 385 kg

to ensure that the vehicle does not become unstable due to rear wheel lock up. The difference in inclination of the green proportioning lines is caused by the difference in COG longitudinal position, wich in turn is caused by the adding of passengers and luggage close to the rear axle. This is also the reason why there is more brake force available on the rear axle than the front axle.

Since the average deceleration requirements are relatively low there is an area of common satisfactory brake force that can be achieved for both the unladen and laden vehicle. The small difference in optimum proportioning makes it possible to develop a combined brake system that can fulfill the legal requirements for service braking regardless of the vehicles load condition.

It is however worth noticing that the results in 4.2.1 are based on the specifications of a prototype vehicle with a driver weight of 75 kg. When the CM EULV reaches its target weight of 120 kg, and if its driven by someone lighter, the area of available brakeforce required for braking at 4.4 m/s^2 will decrease.

In order to determine what dimensions the different brake components should have, the equations from section 2.3.2 and 2.3.3 needs to be used. Because of the large variations in design of drum brakes it is very difficult to establish a mesh showing how the brake force varies depending on its internal measurements. If it is determined that a drum brake is the best option from a brake system setup point of view, a drum brake capable of generating enough brake torque to fulfill the deceleration requirements for a service brake needs to be found. To get some idea of the size to brake force relationship a theoretical model was made using equations 2.3.12 thru 2.3.22, see code in Appendix B. By converting the internal dimensions to functions of the drum radius, introducing a amplification vector on the control force and keeping the angles constant, a graph of resulting brake force could be created. The results are shown in figure 6.2.4 in Appendix A.

A matrix was created to determine appropriate dimensions for components in a hydraulic brake system. This matrix is easier to create since the dimensions of the components are easily determined and are, to some extent, independent of each other. In other words, a certain brake caliper may work on brake discs with different radii, but if an internal dimension of a drum brake is changed the other dimension may or may not change. By using equation 2.3.11 and inserting known variants of master cylinders, brake caliper pistons and brake disc radii a mesh of brake forces is created, see figure 6.2.5 in Appendix A.

By using figure 6.2.5 setups for hydraulic brake systems can be chosen that, given the maximum allowed control force, will generate the correct proportions of brake force. If another dimension of either master cylinder, brake caliper or disc brake is found these are easily entered into the code, see Appendix B.

By using equation 2.3.9 the required road friction coefficient to keep the CM EULV stationary on an 18% incline was calculated. The results are shown in table 4.2.1. Note that unladen weight in this context includes curbweight and the weight of the driver.

The results show that a problem might occur when trying to park the laden CM EULV on an uphill gradient if the parking brake is only applied to the front wheel. This is unfortunate since this implies that the parking brake must act on either both of the axles or on both the rear wheels. This would require both of the rear brakes to have a purely mechanical actuation. If combined hydraulic/mechanical brake calipers are used it is still possible to have a combined hydraulic brake setup. This might also suggest that the main reason for using

Table 4.2.1: Required friction coefficients for parking

	Unladen weight		Laden weight	
	Front	Rear	Front	Rear
Uphill gradient	0.73	0.23	0.96	0.22
Downhill gradient	0.51	0.27	0.60	0.25

a drum brake on the front wheel has disappeared.

4.2.2 Evaluation of physical brake tests

Thru the course of this master thesis all of the prototype vehicles have been tested and evaluated by the authors and by the management at CM. A lot of this driving has occured at locations not suitable for proper brake tests due to lack of space, poor road conditions etc. Even though these testdrives have not generated any concrete data they have accumulated the subjective experiences of the drivers, which are also important to consider. At two separate occasions test have been performed a Volvo Cars test track at Hällered, Sandhult. There the brake performance of P1A and P1B have been tested and results where recorded. The performance of P1D was recorded in the vicinitiy of CM. The weather conditions during the test of P1A were poor, with strong winds and rain. The effect of this will be compensated for in the calculation with a lowered road friction coefficient. The other test were performed during dry road condtions. Due to technical problems the stopping distance of P1C could not be tested. This was unfortunate since this protoype was equipped with control units capable of varying the input power limit to the motors. The recorded data and the corresponding calculated stopping distances can be found in figure 6.2.6 Appendix A. Figure 6.2.6 also shows the recorded stopping distances in contrast to the legal requirements. Note that several results can be present at a single point. The calculated values are done for a interval of lower speeds. This interval occurs because the speedometer, according to information given to CM by EVT, shows a speed between +11% to +16% of the actual speed.

There are a few sources of errors that needs to be recognized. The legal requirements states that the maximum applied control force may not exceed 200 N. There have been no practical way to measure the actual applied control force during the physical tests. The friction coefficient between the brake pad and brake disc or brake drum and linings is also hard to determine and was chosen to be 0.5 after benchmarking different brake pads. It is also very difficult to describe and compare the different vehicles and distances since the conditions changed between the two test days and also during the same test day, with driver changes etc.

Since it is not possible to utilize more brake force than the available traction allows, the first determination for each case needs to be if the available traction or the brake system sets the boundary condition for the deceleration that can be achieved.When the calculations are done for P1A, P1B and P1D according to the theories described in sections 2.3 and 2.3.2 a theoretical stopping distance can be determined and compared to the data from the physical testing. If the measured results are superimposed into the actual speed interval the measured values are generally worse then the calculated. This is of course expected since the model assumes that all the available traction is used perfectly.

Since no physical tests could be performed with the generator brakes on P1C there can only be calculated estimates on stopping distance according to the theory described in subsection 2.3.3. Assuming maximum laden weight and a constant total generator power of 5 kW, figure 6.2.7 shows the estimated stopping distances from various initial velocities. According to these results the current hub motors can not generate enough power to brake the CM EULV according to the legal requirements once the velocity exceeds approximatley 32 km/h. And even if the power input could be increased and varied according to the control force there would still be a problem with the generators low speed torque output. However, this does not disqualify it from interacting with other hydraulic or mechanical brake systems. It only means that it is, in its current form, not a viable option for a separate system.

It was noted that an excessively high control force was necessary in order to halt P1D. In order to get more realistic results, which means control force closer to 200 N, a second series of test was performed were the driver knowingly exerted a lower control force. This series is denoted as ACF in figure 6.2.6 in Appendix A. It is noted that these values better match the ones measured for P1B. The only difference when calculating the stopping distance between the front P1B and P1D is that the latter has a lower total weigth due to the changed rear suspension setup.

Despite the differences between measured and calculated values it can be concluded that all values have been within the legal limits. When further optimization of brake performance is attempted a speedometer with higher precision should be utilized, since a speed difference of 10% translates into an increasing amount of meters in stopping distance. The problem is best demonstrated with the stopping distances for P1A.

4.3 Handling

The results from the calculations regarding handling are presented in figure 4.3.1 where the lateral acceleration is plotted against the longitudinal deceleration. The black lines represent a symmetrically loaded vehicle. The dashed line is the vehicle with driver and the solid line represents the fully laden vehicle. The plot in figure 4.3.1 shows that the cornering capability is slightly improved when the COG is moved back due to increased load in the rear.

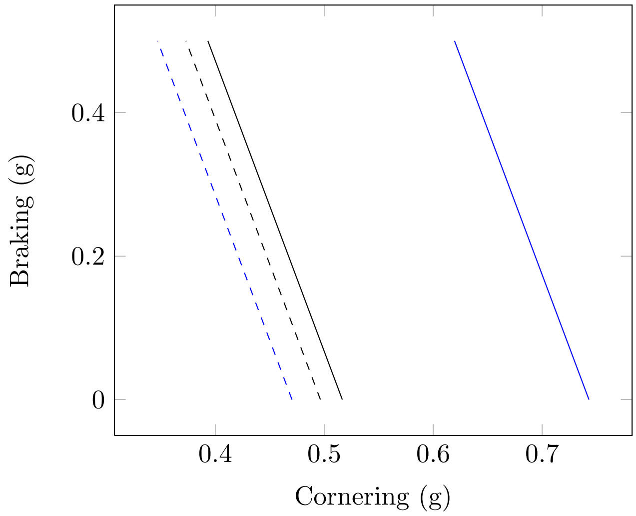

Figure 4.3.1: Limits for combined cornering and braking

The blue lines in the figure demonstrates the effect of asymmetrical loading. The example is calculated with a light driver and a heavy passenger. The dashed line is the result when the passenger is sitting on the wrong side with respect to cornering capability. The solid line, which represents the passenger sitting on the correct side, clearly demonstrates the difference in cornering capability due to vehicle loading.

4.4 Suspension performance

The suspension performance was evaluated both by driving the vehicles and by doing static calculations. For the shock absorber solution the packaging was also examined.

4.4.1 Shock absorber

The design of the shock absorber geometry is a matter of optimization with regards to packaging, cost and weight. A Matlab program was created to derive the optimal mounting points for the suspension with regards to the available space and requirements on maximum allowed forces on the body, see code in Appendix B. The forces induced by vertical loads and lateral accelerations was calculated using the free body diagrams shown in figure 4.4.1. Using coordinates for the upper mounting point of the shock absorber, in relation to swing arm axis, the inclination of the shockabsorber is determined for each set of coordinates of the lower mounting point of the shock absorber. A mesh of the mounting point forces and torques are then generated over an interval of possible lengths of L_{fs}, w and h. The intervals was chosen with regards to the available space. How the forces are distributed to the body will depend on the final design of the inserts. The normal forces and lateral tire forces can be chosen to simulate different load cases.

By implementing constraints on forces, torques, shock absorber lengths, wanted stroke length etc. a subset of suitable mounting positions is found. See figure 6.2.9 in Appendix A for an example of meshes and subsets.

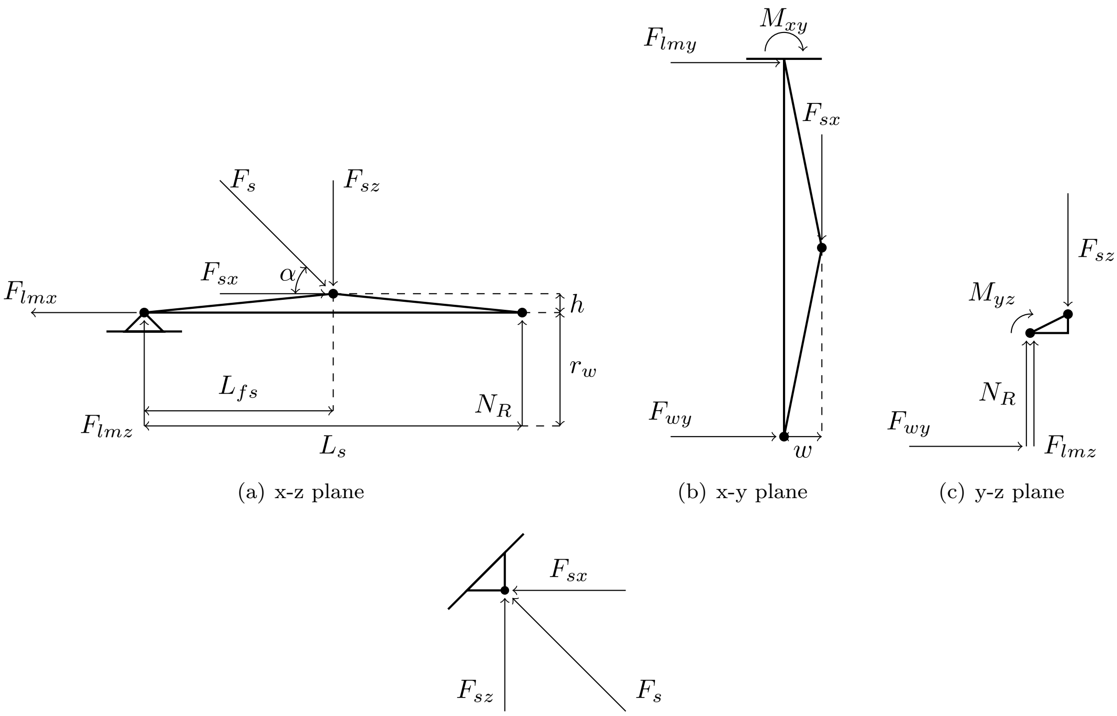

(a) x-z plane

(b) x-y plane

(c) y-z plane

(d) Upper mounting point, x-z plane

Figure 4.4.1: Static model of swing arm and upper mounting point for shock absorber

An attempt was made to find a shock absorber suitable to mount in front of the tire, which would make it a symmetrical monodamper, see figure 4.4.2. This setup was created with the dimension available on P1A, when the swing arm was 400 mm long. The big advantage of this setup is that it would eliminate the torques M_{xy} and M_{yz} due to vertical loads. It also saves space between the rear wheels which allows for a larger luggage compartment. Since packaging was a big issue for this, a Matlab program was created to help determine the possible shock absorber length given available space for lower and upper mounting points. By selecting two wanted points, using pythagoras theorem, the shock absorber length could be determined. Note that this was merely an attempt to find the maximum length as these points might produce direction of forces which are unacceptable with regards to the body. It soon became apparent that this solution suffered from major

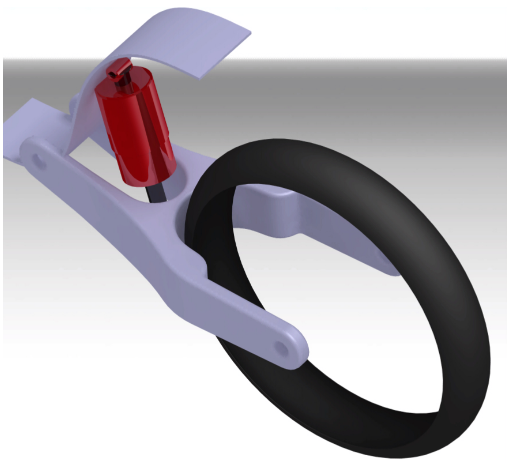

Figure 4.4.2: Packaging-model of monodamper

problems. Even though the torques was eliminated the force F_{sz} was greatly amplified when the distance L_{fs} was decreased. Even if the body could be reinforced to cope with the forces it would be very difficult to find a a shock absorber of suitable length and stiffness.

In order to determine the order of magnitudes of the forces for possible suspension setups the setup on P1B was analysed. The forces in the body caused by the suspension geometry present on P1B during dimensioning conditions and maximum laden weight are presented in table 4.4.1.

Table 4.4.1: Forces and moments in body during dimensioning conditions, shock absorber suspension

Condition	Swing mount: F_x [N]	F_y [N]	F_z [N]	M_x [Nm]	M_z [Nm]	Damper mount: F_x [N]	F_z [N]
Acceleration (0.2 g)	-981	0	-1148	-282	-163	1359	2354
Deceleration (0.5 g)	-493	0	600	-24	-14	116	200
Bump (2.5 g)	-2509	0	-1621	-522	-301	2509	4347
Bump+Deceleration	-2167	0	-114	-254	-147	1222	2116
Cornering (0.5 g)	-2247	-1350	-1452	-197	231	2247	3892
Bump + Cornering	-5618	-3376	-3630	-493	799	5618	9730

The shock absorber suspension setup was tested by driving when mounted on two different vehicles. The first was the three wheel moped purchased for benchmarking purposes. The design of this vehicle was not optimal and this made it very difficult to drive. The main factors contributing to the bad handling was the short trackwidth combined with a relatively high centre of gravity. Such a vehicle, especially when equipped with too soft springs as in this case, will have a large tendency to roll. The driver gets the impression that the vehicle will roll over and it gives a feeling of not being in control.

This same suspension setup was then transferred to the P1B chassis for further evaluation. On this vehicle the setup worked much better thanks to the larger trackwidth and wheelbase. Increasing the pre-tension of the springs gave an improvement but the problem with soft springs still got worse because of the increased weight and the P1B also leaned out too much when cornering. The dampers also reached the bumpstop which caused noise and a jerky suspension behaviour. This was solved by disassembling the damper and replacing the springs with stiffer ones. The standard springs were tested for spring stiffness according to the procedure presented in 3.2.3. The result of the test was a stiffness of 59 N/mm. Based on calculations, the replacement spring stiffness was chosen to be 100 N/mm. A force-deformation diagram for these two sets of springs, at different levels of pre-tension, is represented by the blue and red lines in figure 4.4.3.

The force in the damper caused by the dimensioning condition for vertical acceleration presented in section 1.3 amounts to 5600 N. The diagram shows that it would take even stiffer springs or more pre-tension to meet this demand but this was considered a too large increase in stress for the dampers to handle. Stiffer springs would also increase the risk of sacrificing comfort. The progressive springs mentioned in section 2.5.1 could be a suitable solution to this problem. An example of a force-deformation curve for a progressive spring with a stiffness ranging from 80 to 112 N/mm, at different levels of pre-tension, is presented by the green lines in figure 4.4.3. This indicates a soft behaviour at small deformations with increased stiffness at at large deformations. This type of spring could unfortunately not be tested on the damper used since the spring was too short to get any progressive behaviour.

4.4.2 Rubber suspension axle

The testing of the torsion axle was performed by mounting a section of the axle to a rigid block and measuring the deformation caused by different loads, see subsection 3.2.3. The results from these tests are shown in figure 4.4.4. Two axles with different crossectional dimensions where tested with appropriate size rubber rods with a stiffness of Shore 60A. The blue lines represent the larger axle, using an 80 mm outer pipe, and the red dashed lines represent the smaller axle which uses a 64 mm outer pipe. Each axle was tested at four lengths starting at 330 mm, the original length of the rubber rods, and then shortened with increments of 50 mm. Figure 6.2.8 in Appendix A shows the components. As the axle is made shorter the vertical wheel travel increases for a given load. The results also show that the rubber suspension axle has a progressive behaviour.

The rubber suspension axle was also tested by driving the vehicles fitted with it. The first version was the P1A which had an axle with 400 mm long swingarms. P1A was percieved as unstable during rapid changes of directions and could very easily be manipulated to its roll-over point.

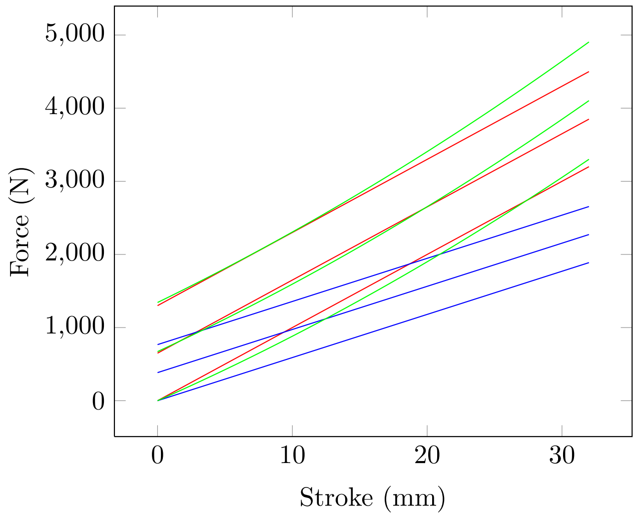

Figure 4.4.3: Constant versus progressive spring stiffness for a damper with a maximum stroke of 32 mm

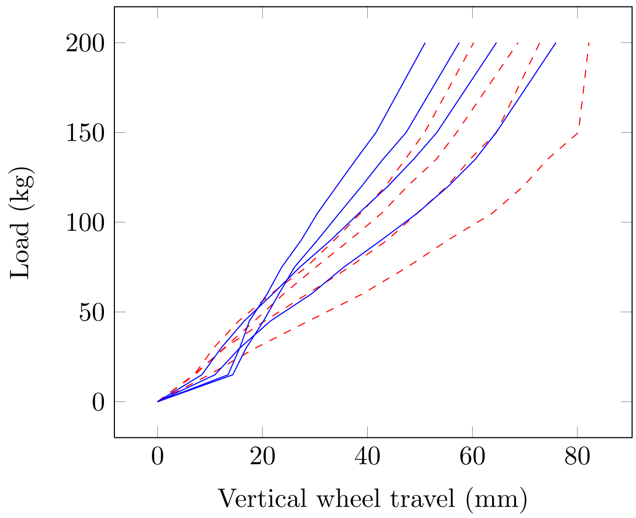

Figure 4.4.4: Measured wheel travel on concept rubber suspension axle

The other vehicle with a rubber suspension axle was P1C. Here the swingarms had been shortened to 280 mm. This means that for the same vertical wheel travel the axle on the P1C had to rotate more, giving more opposing moment in the rubber rods. This made the suspension more responsive and the vehicle felt safer from the drivers point of view.

The forces in the chassis caused by the rubber suspension axle during dimensioning conditions are presented in table 4.4.2.

Table 4.4.2: Forces and moments in body during dimensioning conditions, rubber suspension axle

Condition	M_x [Nm]	M_y [Nm]	M_z [Nm]	F_x [N]	F_y [N]	F_z [N]
Acceleration (0.2 g)	0	-222	0	378	0	1206
Deceleration (0.5 g)	0	-399	0	-945	0	801
Bump (2.5 g)	0	-681	0	0	0	2725
Bump+Deceleration	0	-699	0	-945	0	2002
Cornering (0.5 g)	284	-610	338	0	1350	2700
Bump+Cornering	709	-1525	844	0	3376	6751

4.5 Anti-roll bar performance

The calculations done on the anti-roll bar show that only a limited effect can be achieved when mounted on the rubber suspension axle. The design of this suspension setup limits the diameter of the bar to 13 mm and since it must be fastened on both sides of the suspension it must be 1220 mm long. The calculated effect of an anti-roll bar fulfilling these restrictions is shown in figure 4.5.1. The dashed and solid lines represent the vehicle with and without anti-roll bar at the prescribed loadcases. The weight of this bar is approximately 1.3 kg.

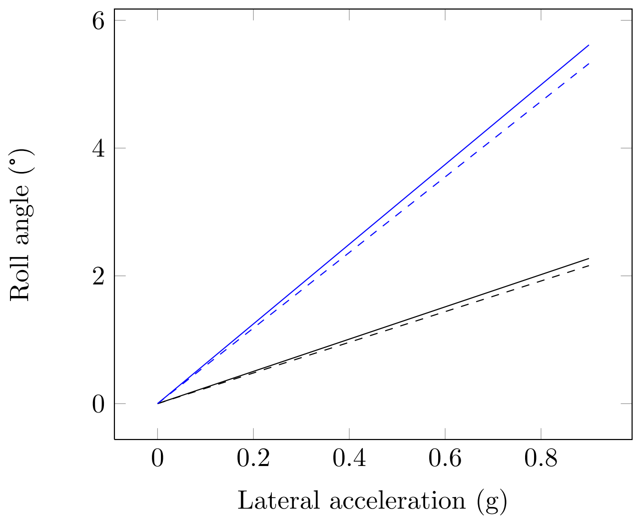

Figure 4.5.1: Effects of solid anti-roll bar; diameter 13 mm, length 1220 mm

Greater effect with less weight can be achieved with the split suspension concepts where the space between the swingarm axes is unoccupied. It would then be possible to mount a shorter bar with larger diameter, two factors that both increase the stiffness of the bar. An example is shown in figure 4.5.2 where a 0.5 m long circular tube is simulated. The tube is 20 mm in diameter and the material thickness is 2 mm. This tube weighs 0.45 kg which is approximately one third of the solid bar shown in figure 4.5.1 and at the same time it gives more roll reduction.

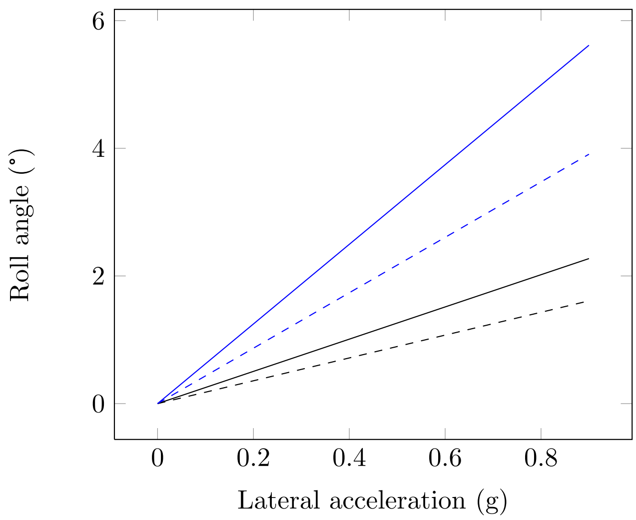

Figure 4.5.2: Effects of tube anti-roll bar; outer diameter 20 mm, wall thickness 2mm and length 500 mm

The physical testing of the anti-roll bar was carried out with a vehicle fitted with the rubber suspension axle. The anti-roll bar was a solid circular bar, 13 mm in diameter and 1220 mm long as demonstrated in figure 4.5.1. The vehicle was driven both with and without the anti-roll bar for comparison.

The regular driving gave a somewhat negative impression. The effect of the anti-roll bar is limited for the small roll angles experienced when the vehicle is not pushed hard. The impression is instead that it adds a disturbance to the handling during regular driving.

On the skidpad P1C was driven at maximum speed using only one motor, due to technical problems, at a slowly decreasing turn radius and without the anti-roll bar fitted. The turn radius negotiable without lifting the inner wheel was 11 m. The same test was then performed with the anti-roll bar and this time the radius shrunk to below 9 m.

5 Conclusions

The conclusions are based on the results from the static calculations, physical testing and overall experiences accumulated during the making of this thesis.

5.1 Brakes

The choice of brake system is primarily a question of fulfilling the legal requirements. Thereafter factors such as cost, weight and brake operation can be considered. The requirements can be fulfilled in numerous ways but not all the systems presented are in accordance with the other design constraints. The cost is kept low by chosing a system with low complexity and few components. Few components are also advantageous for the weight.

The brake actuation was evaluated during testing and the results showed that properly dimensioned hydraulic disc brakes have the best performance. Using the motors for braking also felt good from a drivers point of view. The performance of the drum brake on P1B and P1D inspired little confidence and required a high control force. Its only advantage is that it is purely mechanical and can therefore be used as a parking brake. Even though the results from the physical testing show that the stopping distances are in accordance with the legal requirements, a solution containing a drum brake can not be recommended for the CM EULV.

There is also a question of whether to use a combined or separated system. The combined is easiest for the driver while the separated reduces cost and complexity.

The combined experience of the results leads to two concepts which both fulfills the legal requirements but have different setups. If combined hydraulic/mechanical brake calipers of appropriate size can be found a combined brake system is the best option. This is because it benefits the driver while keeping the number of components low. This also means that the parking brake actuator can be placed somewhere other than the handlebars since it will not be used as a service brake. The cost might however be higher since these calipers are not that common. Electrical braking can also be implemented on top of this system. Had the difference in brake proportioning due to load been larger this would not have been an suitable system without extra control systems. If combined hydraulic/mechanical brake calipers of reasonable size and cost can not be found a separate system is recommended, where the front brake system is a hydraulic disc brake and the rear brakes are mechanically operated disc-brakes which also functions as parking brake. The front brake handle brake light switch should also engage the electrical brake. This system is slightly more complex but uses more common components. The difference in cost will largely depend on the cost of the proposed combined brake calipers.

5.2 Suspension

The test driving showed that both suspension concepts are realistic alternatives that can be used for the final vehicle. The two solutions present different characteristics and both have positive and negative properties. During the test drives it also became apparent that the tires have a major influence on the handling of the vehicle. This is another factor that can be altered in order to optimize the vehicle. It might also be a way of reducing the risk of the vehicle rolling over if the tires start to slide before they generate enough force to roll the vehicle over. This choice must of course be made with regards to other factors such as safety and rolling resistance of the tires.

When recommending a suspension concept to be used on the final vehicle many factors must be considered. The design and packaging of the rubber suspension axle clearly has greater potential since the whole construction can be hidden inside the body with only the swingarms visible. The cost of this setup is lower since it only consists of the two pipes and the rubber rods, not including the swing arms since these are used in both concepts. The weight is probably similar between the concepts but the rubber suspension axle has a greater potential for saving weight since the current model is overdimensioned and made entirely out of steel.

The shock absorber concept shows better performance in handling when the vehicle is pushed to its limits. It gives better feedback to the driver and it behaves in a more predictable way. The rubber suspension axle gives a smoother ride but the chassis tends to move around more when pushing the boundaries. The consequence of this is that the shock absorbers are less comfortable during regular driving when the suspension can be a bit jerky. This effect might be possible to reduce by optimizing the shock absorber settings and the spring stiffness. The predictable behaviour of the springs and dampers means they can be optimized by doing static calculations which is much more difficult for the rubber suspension axle due to the nonlinear behaviour of the rubber material.

The anti-roll bar improved the cornering capacity when pushing the vehicle to the limit but had little effect during regular driving. The weight and cost added by the anti-roll bar is therefore considered not to be worth the slight improvement in vehicle dynamics.

The main conclusion regarding the suspension is that the rubber suspension axle is better suited for the CM EULV. The vehicle has a top speed of 45 km/h and is intended for commuter trips and short distance urban transportation. This means that for the customer the high speed performance is less important than the price and comfort of the vehicle. The potential for saving weight is also important since reduced weight improves all aspects of the vehicle.

6 Future work

This chapter consists of the authors recommendations for continued work regarding the areas studied in this thesis.

6.1 Brakes

The next step for the brake system concept is complete physical testing according to the legal requirements with the complete system. The system must be tested to make sure that the components works together and the interface between driver and brake system must also be evaluated. Since the P1C is equipped with a control system for braking electrically it would be interesting to measure the braking performance when using electrical braking only.

An evaluation of methods of locking the CM EULV while parked needs to be performed. The challenge is to make the vehicle difficult to move while parked. This means a suitable system to lock the parking brake needs to be developed, preferably one which is not too complex.

6.2 Suspension

Further testing needs to be done on the split rubber suspension axle described in this thesis. This testing would require that a proper test rig is constructed and a matrix of load cases is determined and performed on a series of axles. In order to optimize both the behaviour of the axle and the dimension of individual components this testing could be combined with FEM simulations.

A simplified FEM model was set up during this thesis but no results could be extracted. The model represented only a quarter of a crossection of the rubber suspension axle to minimize the computing time. The pre-processor ANSA was used to set up the geometry and mesh it. The LS-DYNA deck of ANSA was used to apply loads, constraints and material properties. The pipes were modelled as rigid while the rubber rod was modelled using the Ogden hyperelastic material model. The simulation consisted of two separate steps to account for the pre-tension of the rubber. The first step modelled the compression of the rubber between the two pipes and in the second step the inner pipe was applied with a moment to simulate the rotation of the swing arm. Because of the large deformations in the rubber, the model did not work properly and could not provide any results. If working properly, with the correct material properties for the rubber used and matched against the physical tests performed on the rubber suspension axle, this type of model could be used for numerous purposes. These include both the split axle as well as the standard design. The simplified model could be used to model rubber rods and pipes of different sizes. The stresses in the pipes could also be calculated. By expanding the model, more effects could be taken into account, such as the free ends of the rubber rods. A complete model could also provide the bending moments induced in the axle.

Appendix A

Table 6.2.1: P1A Specifications

Prototype 1A	Type	Item	Dimension
Unladen mass			160 kg
Brake system			
	Front, Hydraulic		
		Master cylinder ∅	14 mm
		Single piston caliper ∅	30 mm
		Brake disc ∅	160 mm
		Handbrake lever	150/30 mm
	Rear, N/a		
Rear suspension			
	Rubber suspension axle		
		Svingarm length	400 mm
Propulsion			
		EVT- Scooter 4000e e	1x 1.5 kW

Table 6.2.2: P1B Specifications

Prototype 1B	Type	Item	Dimension
Unladen mass			195.6 kg
Brake system			
	Front, Mechanical		
		Drum brake ∅	120 mm
		Handbrake lever	120/30 mm
	Rear, Hydraulic		
		Master cylinder ∅	14 mm
		2 single piston calipers ∅	30 mm
		Brake disc ∅	180 mm
		Handbrake lever	150/30 mm
Rear suspension			
	Shockabsorber suspension		
		Spring stiffness	59 N/mm
		Svingarm length	280 mm
Propulsion			
		EVT- Scooter 4000 e	2 x 1.5 kW

Table 6.2.3: P1C Specifications

Prototype 1C	Type	Item	Dimension
Unladen mass			171.6 kg
Brake system			
	Front, Hydraulic		
		Master cylinder ∅	14 mm
		Single piston calipers ∅	30 mm
		Brake disc ∅	155 mm
		Handbrake lever	150/30 mm
	Rear, Electric Generator		
Rear suspension			
	Rubber suspension axle		
		Svingarm length	280 mm
Propulsion			
		Kelly electrics	2 x 2 kW

Table 6.2.4: P1D Specifications

Prototype 1D	Type	Item	Dimension
Unladen mass			190.2 kg
Brake system			
	Front, Mechanical		
		Drum brake ∅	120 mm
		Handbrake lever	120/30 mm
	Rear, Hydraulic		
		Master cylinder ∅	14 mm
		2 single piston calipers ∅	30 mm
		Brake disc ∅	180 mm
		Handbrake lever	150/30 mm
Rear suspension			
	Rubber suspension axle		
		Swingarm length	280 mm
Propulsion			
		EVT- Scooter 4000 e	2 x 1.5 kW

Figure 6.2.1: Rubber suspension axle on P1A

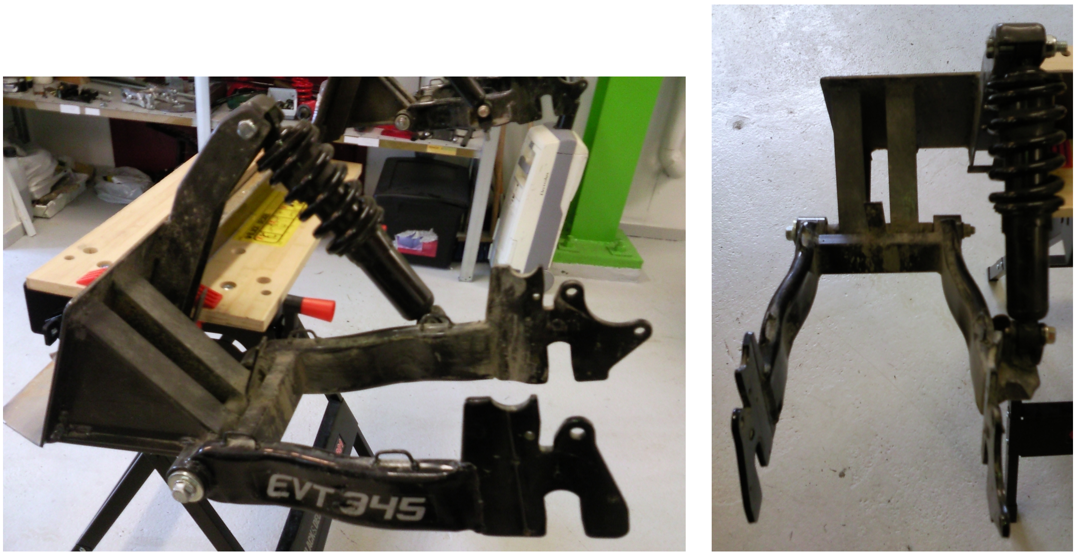

Figure 6.2.2: Placement of shockabsorber on P1B

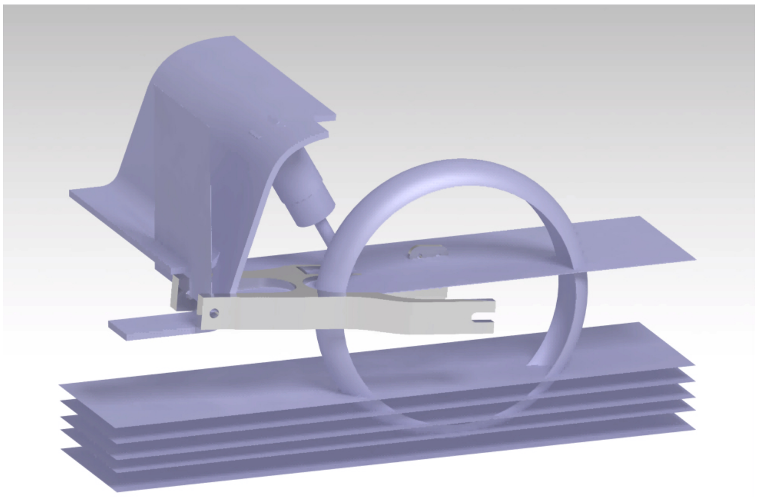

Figure 6.2.3: CAD dimensioning model

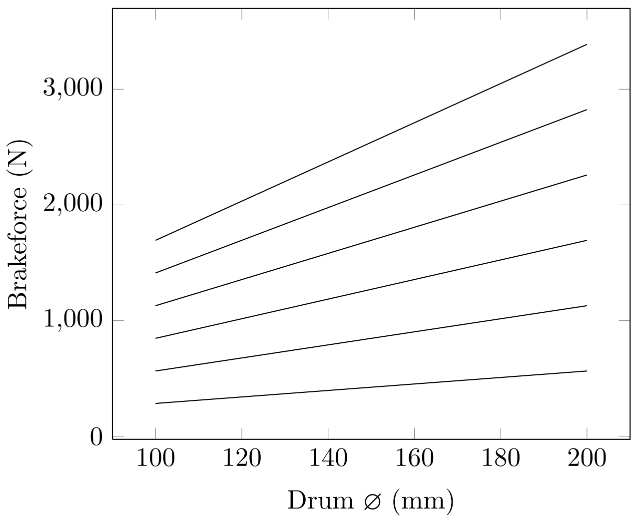

Figure 6.2.4: Brake force for drum brake with increasing diameter and control force amplification

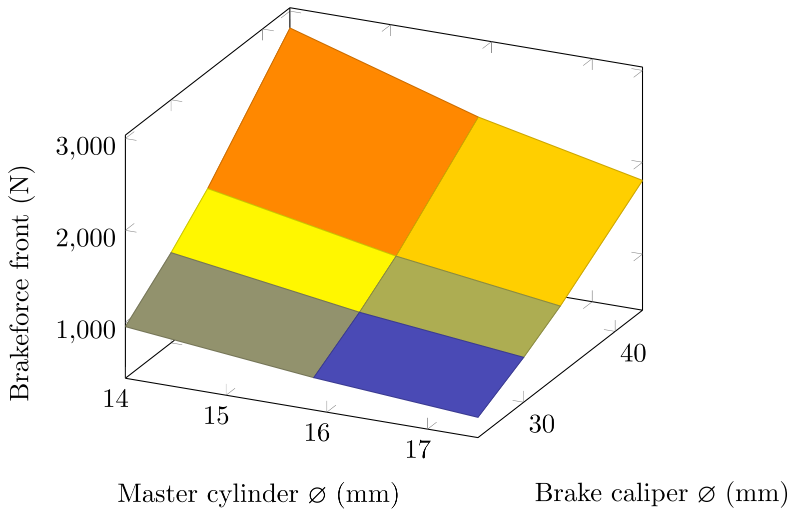

(a) Brake force of 2 piston calipers with outer disc diameter 150 mm and wheel radius 0.215 m

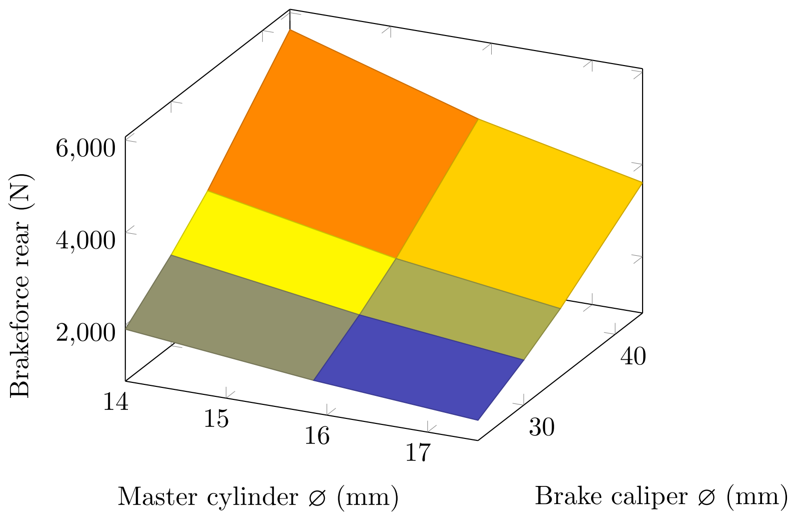

(b) Brake force of double 2 piston calipers with outer disc diameter 150 mm and wheel radius 0.215 m

Figure 6.2.5: Brake forces as functions of controlforce, master cylinder diameter, brake caliper piston diameter, brake disc- diameter and wheel-radius

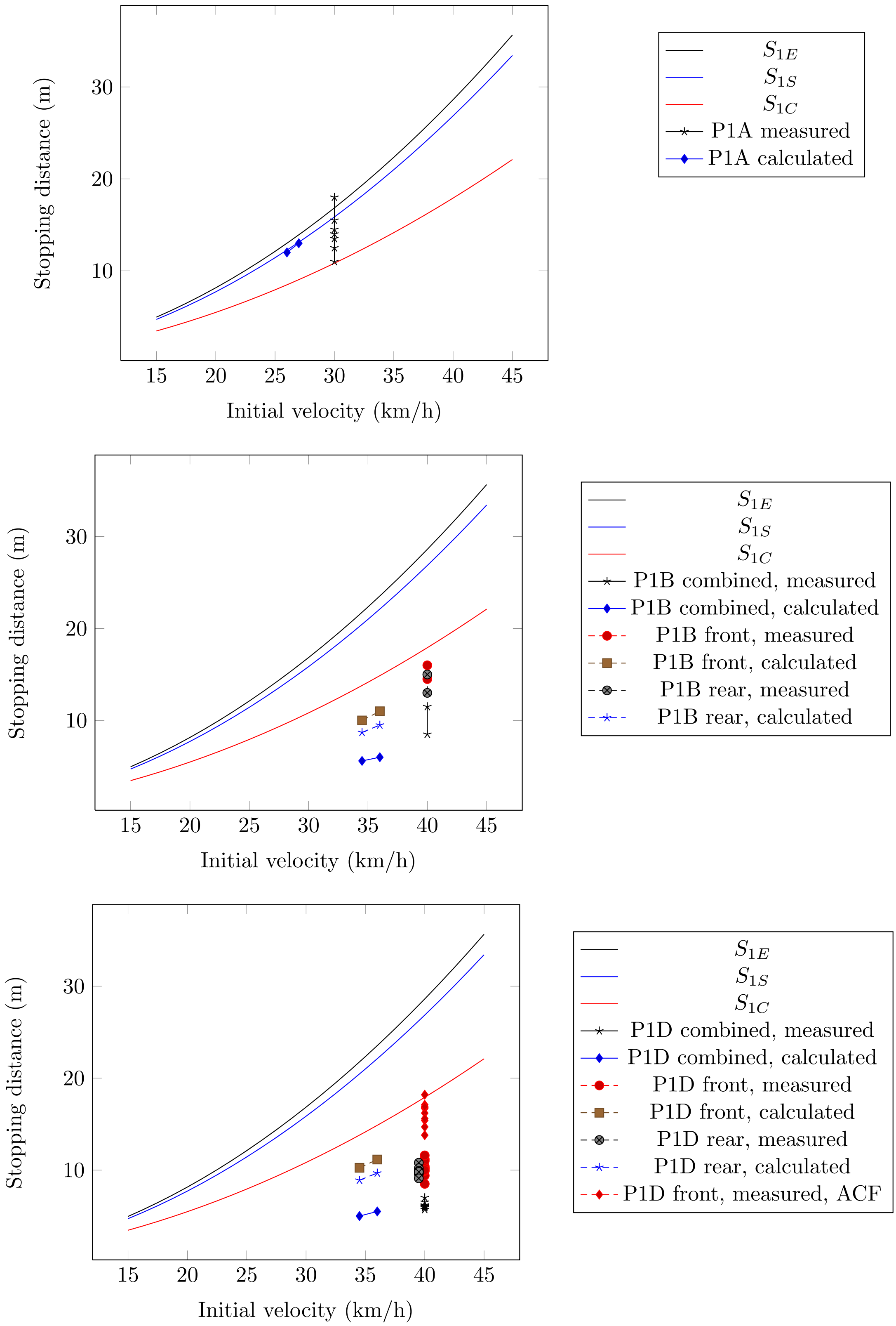

Figure 6.2.6: Recorded stopping distances for P1A, P1B and P1D

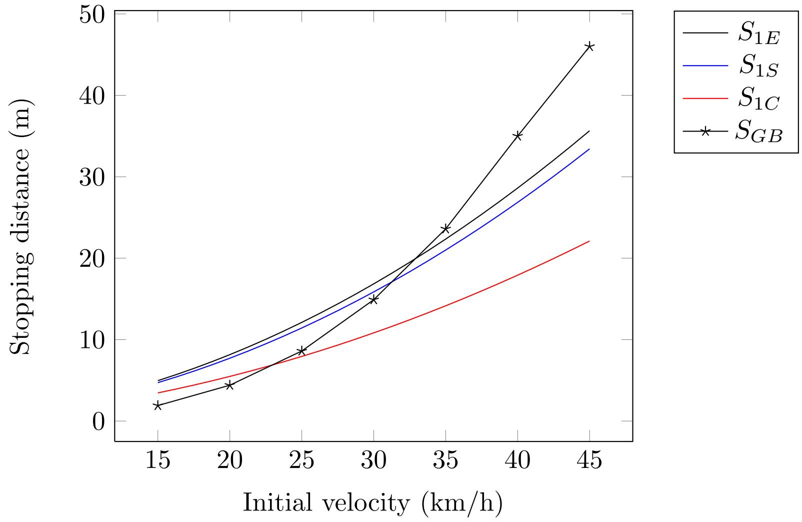

Figure 6.2.7: Estimated stopping distances for generator brakes at 385 kg and 5 kW

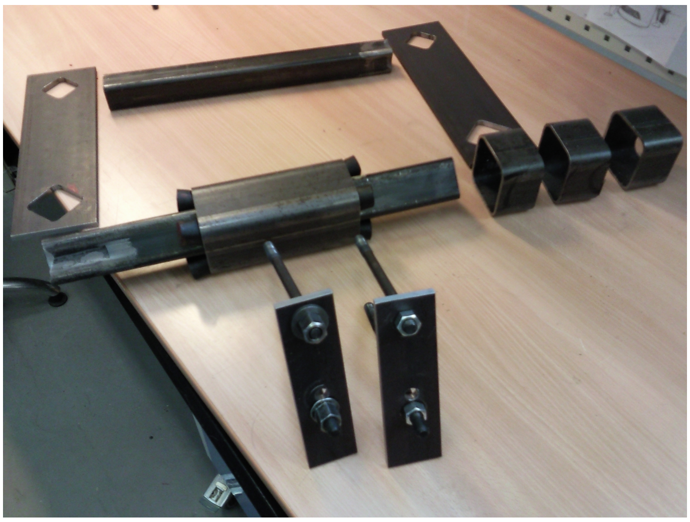

Figure 6.2.8: Parts of testrigg with the cut-off segments

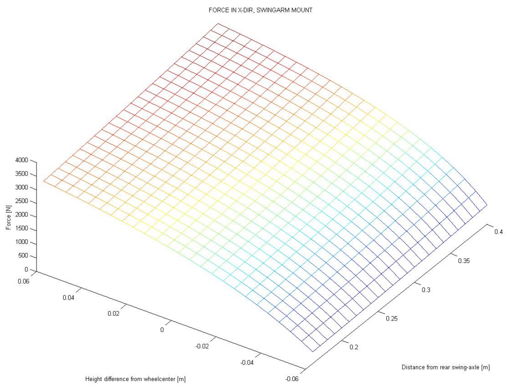

(a) Forces in x-direction, swingarm mount

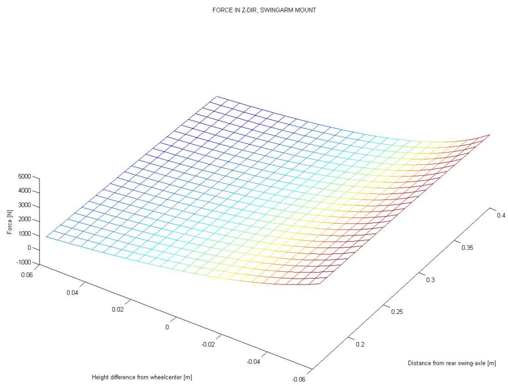

(b) Forces in z-direction, swingarm mount

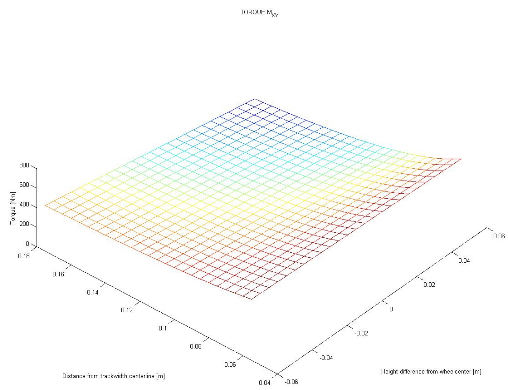

(c) Torque M_{xy}, swingarm mount

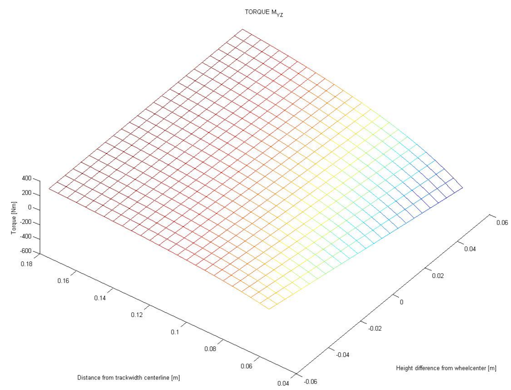

(d) Torque M_{yz}

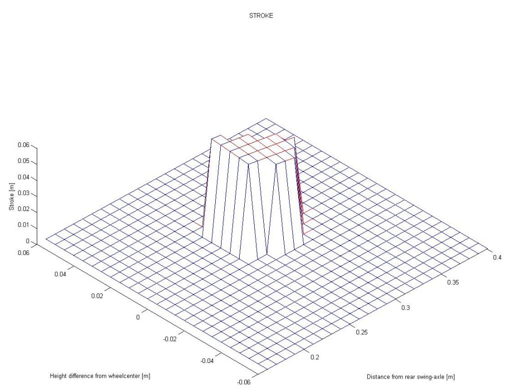

(e) Shockabsorber stroke length

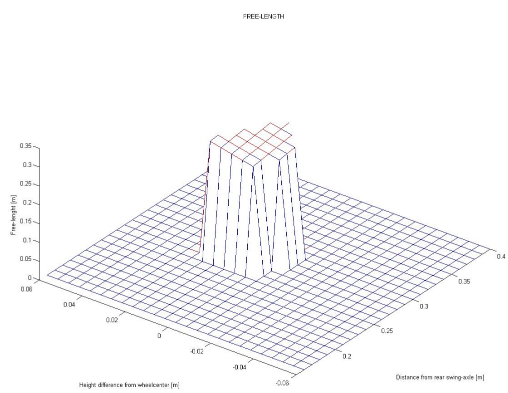

(f) Shockabsorber free length

Figure 6.2.9: Resulting meshes of Matlab code "Forces on body" in Appendix B

Appendix B

```
%CENTER OF GRAVITY
clear all
clc
clf

g = 9.82;
rw = 0.2;    % [m] radius wheel
tw = 1;      % [m] track width

%mass of parts [kg], w = wheel, s = suspension, ba = battery,
%bo = body, d = driver, p = passenger, l = luggage
mwf = 5;
msf = 5.5;
mba = 22;
mbo = 72;
msr = 26;
mwr = 31.2;

md = [35:5:75];
mp = [35:5:75];
m2p = [70:10:150];
ml = 5;

m_vec =[mwf msf mba mbo msr mwr];
mcurb = sum(m_vec);

mcurb_w = 160;

%lengths [m], CATIA measurements, prototype 1B
Ltot = 1.963;

lws = 0.155;
lsb = 0.763;
lbc = 0.202;
lca = 0.509;
lae = 0.334;

ldx = 0.973;
lpx = 1.955;
llx = 1.963;

l_vec =[lws; lsb; lbc; lca; lae];

if Ltot ~= sum(l_vec)
    disp('OBS!! Ltot unequal to L_vec');
end

lf_unl = (lae*mwr+lca*(msr+mwr)+lbc*(mbo+msr+mwr)+lsb*(mcurb-mwf-msf)...
+lws*(mcurb-mwf))/mcurb;

%heights [m], CATIA measurements, prototype 1B
htot = 0.403;

hwe = 0.046;
```

```
heb = 0.089;
hbs = 0.134;
hsc = 0.134;

hd = 0.642;
hp = 0.505;
hl = 0.1;

h_vec =[hwe; heb; hbs; hsc];

if htot ~= sum(h_vec)
    disp('OBS!! htot unequal to h_vec');
end

h_ur = (mbo*htot+msf*(htot-hsc)+mba*(hwe+heb)+msr*hwe)/mcurb;

h_unl = h_ur+rw;

%passenger lateral displacement from centerline
yp = 0.28;

COG_UNL = [lf_unl,0,h_unl];

%vehicle with driver
for i = 1:9
    lf_ld(i) = (mcurb*lf_unl+md(i)*ldx)/(md(i)+mcurb);
    h_ld(i) = (h_ur*mcurb+md(i)*hd)/(md(i)+mcurb)+rw;
end

  COG_ld = [lf_ld; h_ld];

%location of COG with passengers and luggage
for i = 1:9
    for j = 1:9
    %vehicle with driver and 1 passenger with luggage
lf_ldpl(i,j) = (mcurb*lf_unl+md(i)*ldx+mp(j)*lpx+ml*llx)...
    /(mcurb+md(i)+mp(j)+ml);
h_ldpl(i,j)=(h_ur*mcurb+hd*md(i)+hp*mp(j)+hl*ml)/(mcurb+md(i)+mp(j)+ml)+rw;
y_ldpl(i,j) = mp(j)*yp/(mcurb+md(i)+mp(j)+ml);

    %vehicle with driver and 1 passenger without luggage

lf_ldp(i,j) = (mcurb*lf_unl+md(i)*ldx+mp(j)*lpx)/(mcurb+md(i)+mp(j));
h_ldp(i,j) = (h_ur*mcurb+hd*md(i)+hp*mp(j))/(mcurb+md(i)+mp(j))+rw;
y_ldp(i,j) = mp(j)*yp/(mcurb+md(i)+mp(j));

     %vehicle with driver and 2 passengers with same weight with luggage

lf_ldppl(i,j) = (mcurb*lf_unl+md(i)*ldx+m2p(j)*lpx+ml*llx)...
    /(mcurb+md(i)+m2p(j)+ml);
h_ldppl(i,j) = (h_ur*mcurb+hd*md(i)+hp*m2p(j)+hl*ml)...
    /(mcurb+md(i)+m2p(j)+ml)+rw;

     %vehicle with driver and 2 passengers with same weight without luggage

lf_ldpp(i,j) = (mcurb*lf_unl+md(i)*ldx+m2p(j)*lpx)/(mcurb+md(i)+m2p(j));
```

```
h_ldpp(i,j) = (h_ur*mcurb+hd*md(i)+hp*m2p(j))/(mcurb+md(i)+m2p(j))+rw;
    end
end

% REMOVE ; IN ORDER TO SEE COG FOR EACH SET
for i = 1:9
    p = [1:9];
    COG_ldpl = [lf_ldpl(i,p); y_ldpl(i,p); h_ldpl(i,p)];
    COG_ldp = [lf_ldp(i,p); y_ldp(i,p); h_ldp(i,p)];
    COG_ldppl = [lf_ldppl(i,p); h_ldppl(i,p)];
    COG_ldpp = [lf_ldpp(i,p); h_ldpp(i,p)];
end

%NORMAL FORCES, SCENARIOS (SYMMETRICAL)
 %   1. ONLY LIGHT DRIVER 2. LIGHT DRIVER WITH HEAVY PASSENGERS AND LUGGAGE
  %  3. ONLY HEAVY DRIVER 4. HEAVY DRIVER,HEAVY PASSENGERS,LUGGAGE

m = [mcurb+md(1) mcurb+md(1)+m2p(9)+ml mcurb+md(9) mcurb+md(9)+m2p(9)+ml];
lf = [lf_ld(1) lf_ldppl(1,9) lf_ld(9) lf_ldppl(9,9)];
h = [h_ld(1) h_ldppl(1,9) h_ld(9) h_ldppl(9,9)];

m = [195 350];
lf = [1.2 1.4];
h = [0.54 0.6];
a = [0:1:5];

    for i = 1:length(m)
        for j = 1:length(a)
            Nf(i,j) = (m(i)*(g*(Ltot-lf(i))+a(j)*h(i)))/Ltot;
            Nr(i,j) = (m(i)*(g*lf(i)-a(j)*h(i)))/Ltot;

            Fbf(i,j) = Nf(i,j)*1;
            Fbr(i,j) = Nr(i,j)*1;
        end
    end

figure(2)
hold on
title('SYMMETRICAL LOAD')
xlabel('Deceleration [m/s^2]')
ylabel('Available brakeforce on road [N]')
% leg1 = legend('LD','LDHPPL','HD','HDHPPL');
%set(leg1,'Location','Best');
axis([0 5 0 3500])
plot(a,Fbf,'--')
plot(a,Fbr,'.-')

% STRAIGHT-LINE BRAKING WITH ASYMMETRICAL LOAD,
% MAXIMUM LATERAL DISPLACEMENT OF COG

alpha = atan(tw/(2*Ltot));
ro = tw*cos(alpha);
ytot = lf_ldpl(1,9)*tan(alpha);
omega = (ytot-y_ldpl(1,9))*cos(alpha);

for i = 1:length(a)
```

```
   Nrl(i)=((mcurb+md(1)+mp(9)+ml)*(g*omega-a(i)*sin(alpha)*h_ldpl(1,9)))/ro;
end

a_sb = (g*omega)/(sin(alpha)*h_ldpl(1,9));

figure(3)
hold on
title('STRAIGHT-LINE BRAKING WITH ASYMMETRICAL LOAD')
xlabel('Deceleration [m/s^2]')
ylabel('Normal force on rear wheel opposite of centerline [N]')
axis([0 20 0 1000])
plot(a,Nrl,'.-')

%PARKING BRAKE, 18% INCLINE
alphap=18; %by law required inclination in percent
alpha=atand(alphap/100); %required angle in degrees
Afp=0.0014;
mybd = 0.6;
r=0.0725;
for i = 1:9
    Nreq_ld(i) = (mcurb+md(i))*g*sind(alpha);
    Nf_ld(i) = (mcurb+md(i))*g*cosd(alpha)-((mcurb+md(i))*g*cosd(alpha)...
        *lf_ld(i)+Nreq_ld(i)*h_ld(i))/Ltot;
    Nr_ld(i) = (mcurb+md(i))*g-Nf_ld(i);
    myrf_ld(i) = Nreq_ld(i)/Nf_ld(i);
    myrr_ld(i) = Nreq_ld(i)/Nr_ld(i);
end
for i = 1:9
     for j = 1:9
Nreq_ldpl(i,j) = (mcurb+md(i)+mp(j)+ml)*g*sind(alpha);
%required force between braking wheel and ground
Nf_ldpl(i,j) = (mcurb+md(i)+mp(j)+ml)*g*cosd(alpha)-((mcurb+md(i)+mp(j)+ml)...
    *g*cosd(alpha)*lf_ldpl(i,j)+Nreq_ldpl(i,j)*h_ldpl(i,j))/Ltot;
Nr_ldpl(i,j) = (mcurb+md(i)+mp(j)+ml)*g-Nf_ldpl(i,j);
%normal force at rear wheel (front wheel above)
myrf_ldpl(i,j) = Nreq_ldpl(i,j)/Nf_ldpl(i,j);
%required friction coefficient when braking front wheel
myrr_ldpl(i,j) = Nreq_ldpl(i,j)/Nr_ldpl(i,j);
%required friction coefficient when braking rear wheels

Nreq_ldp(i,j) = (mcurb+md(i)+mp(j))*g*sind(alpha);
Nf_ldp(i,j) = (mcurb+md(i)+mp(j))*g*cosd(alpha)-((mcurb+md(i)+mp(j))...
    *g*cosd(alpha)*lf_ldp(i,j)+Nreq_ldp(i,j)*h_ldp(i,j))/Ltot;
Nr_ldp(i,j) = (mcurb+md(i)+mp(j))*g-Nf_ldp(i,j);
myrf_ldp(i,j) = Nreq_ldp(i,j)/Nf_ldp(i,j);
myrr_ldp(i,j) = Nreq_ldp(i,j)/Nr_ldp(i,j);

Nreq_ldppl(i,j) = (mcurb+md(i)+m2p(j)+ml)*g*sind(alpha);
Nf_ldppl(i,j) = (mcurb+md(i)+m2p(j)+ml)*g*cosd(alpha)-((mcurb+md(i)+m2p(j)...
    +ml)*g*cosd(alpha)*lf_ldppl(i,j)+Nreq_ldppl(i,j)*h_ldppl(i,j))/Ltot;
Nr_ldppl(i,j) = (mcurb+md(i)+m2p(j)+ml)*g-Nf_ldppl(i,j);
myrf_ldppl(i,j) = Nreq_ldppl(i,j)/Nf_ldppl(i,j)
myrr_ldppl(i,j) = Nreq_ldppl(i,j)/Nr_ldppl(i,j)

Nreq_ldpp(i,j) = (mcurb+md(i)+m2p(j))*g*sind(alpha);
Nf_ldpp(i,j) = (mcurb+md(i)+m2p(j))*g*cosd(alpha)-((mcurb+md(i)+m2p(j))...
```

```
    *g*cosd(alpha)*lf_ldpp(i,j)+Nreq_ldpp(i,j)*h_ldpp(i,j))/Ltot;
Nr_ldpp(i,j) = (mcurb+md(i)+m2p(j))*g-Nf_ldpp(i,j);
myrf_ldpp(i,j) = Nreq_ldpp(i,j)/Nf_ldpp(i,j);
myrr_ldpp(i,j) = Nreq_ldpp(i,j)/Nr_ldpp(i,j);
    end
end

%CORNERING
beta=atand(tw/2/Ltot);%angle between centerline and line between front
%                      and rear wheel
for i = 1:9
ag_ld(i)=lf_ld(i)*sind(beta)/h_ld(i); %accepted g in lateral acceleration
end
for i = 1:9
    for j = 1:9
ag_ldpl1(i,j)=(lf_ldpl(i,j)*sind(beta)-y_ldpl(i,j)*cosd(beta))/h_ldpl(i,j);
%accepted g with passenger on nonpreferred side
ag_ldpl2(i,j)=(lf_ldpl(i,j)*sind(beta)+y_ldpl(i,j)*cosd(beta))/h_ldpl(i,j);
%accepted g with passenger on preferred side

ag_ldp1(i,j)=(lf_ldp(i,j)*sind(beta)-y_ldp(i,j)*cosd(beta))/h_ldp(i,j);
ag_ldp2(i,j)=(lf_ldp(i,j)*sind(beta)+y_ldp(i,j)*cosd(beta))/h_ldp(i,j);

ag_ldppl(i,j)=lf_ldppl(i,j)*sind(beta)/h_ldppl(i,j);

ag_ldpp(i,j)=lf_ldpp(i,j)*sind(beta)/h_ldpp(i,j);
    end
end

%CORNERING WITH LOAD TRANSFER AND BRAKING WHILE CORNERING
K=30000; %spring stiffness
Kphi=K*tw^2/2; %roll stiffness
brg=0.5; %braking g
brgplot = [0:0.5:0.5];
for i = 1:9
phi=Nr_ld(i)*ag_ld(i)*h_ld(i)/(Kphi-Nr_ld(i)*h_ld(i));
aglt_ld(i)=(lf_ld(i)*sind(beta)-h_ld(i)*tan(phi))/h_ld(i);
%accepted g in lateral acceleration
agltbc_lp(i)=(lf_ld(i)*sind(beta)-h_ld(i)*tan(phi))/h_ld(i)-brg*sind(beta);
%accepted g in lateral acceleration with added braking
end
for i = 1:9
    for j = 1:9
phi_ldpl1(i,j)=Nr_ldpl(i,j)*ag_ldpl1(i,j)*h_ldpl(i,j)/...
    (Kphi-Nr_ldpl(i,j)*h_ldpl(i,j)); %roll angle
aglt_ldpl1(i,j)=(lf_ldpl(i,j)*sind(beta)-y_ldpl(i,j)*cosd(beta)-h_ldpl(i,j)...
    *tan(phi_ldpl1(i,j)))/h_ldpl(i,j);
%accepted g with passenger on nonpreferred side
agltbc_ldpl1(i,j)=(lf_ldpl(i,j)*sind(beta)-y_ldpl(i,j)*cosd(beta)...
    -h_ldpl(i,j)*tan(phi_ldpl1(i,j)))/h_ldpl(i,j)-brg*sind(beta);

phi_ldpl2(i,j)=Nr_ldpl(i,j)*ag_ldpl2(i,j)*h_ldpl(i,j)/...
    (Kphi-Nr_ldpl(i,j)*h_ldpl(i,j));
aglt_ldpl2(i,j)=(lf_ldpl(i,j)*sind(beta)+y_ldpl(i,j)*cosd(beta)...
    -h_ldpl(i,j)*tan(phi_ldpl2(i,j)))/h_ldpl(i,j);
%accepted g with passenger on preferred side
```

```
agltbc_ldpl2(i,j)=(lf_ldpl(i,j)*sind(beta)+y_ldpl(i,j)*cosd(beta)...
    -h_ldpl(i,j)*tan(phi_ldpl2(i,j)))/h_ldpl(i,j)-brg*sind(beta);

phi_ldp1(i,j)=Nr_ldp(i,j)*ag_ldp1(i,j)*h_ldp(i,j)/...
    (Kphi-Nr_ldp(i,j)*h_ldp(i,j));
aglt_ldp1(i,j)=(lf_ldp(i,j)*sind(beta)-y_ldp(i,j)*cosd(beta)...
    -h_ldp(i,j)*tand(phi_ldp1(i,j)))/h_ldp(i,j);
agltbc_ldp1(i,j)=(lf_ldp(i,j)*sind(beta)-y_ldp(i,j)*cosd(beta)...
    -h_ldp(i,j)*tan(phi_ldp1(i,j)))/h_ldp(i,j)-brg*sind(beta);

phi_ldp2(i,j)=Nr_ldp(i,j)*ag_ldp2(i,j)*h_ldp(i,j)...
    /(Kphi-Nr_ldp(i,j)*h_ldp(i,j));
aglt_ldp2(i,j)=(lf_ldp(i,j)*sind(beta)+y_ldp(i,j)*cosd(beta)...
    -h_ldp(i,j)*tand(phi_ldp2(i,j)))/h_ldp(i,j);
agltbc_ldp2(i,j)=(lf_ldp(i,j)*sind(beta)+y_ldp(i,j)*cosd(beta)...
    -h_ldp(i,j)*tan(phi_ldp2(i,j)))/h_ldp(i,j)-brg*sind(beta);

phi_ldppl(i,j)=Nr_ldppl(i,j)*ag_ldppl(i,j)*h_ldppl(i,j)...
    /(Kphi-Nr_ldppl(i,j)*h_ldppl(i,j));
aglt_ldppl(i,j)=(lf_ldppl(i,j)*sind(beta)-h_ldppl(i,j)...
    *tand(phi_ldppl(i,j)))/h_ldppl(i,j);
agltbc_ldppl(i,j)=(lf_ldppl(i,j)*sind(beta)-h_ldppl(i,j)...
    *tan(phi_ldppl(i,j)))/h_ldppl(i,j)-brg*sind(beta);

phi_ldpp(i,j)=Nr_ldpp(i,j)*ag_ldpp(i,j)*h_ldpp(i,j)...
    /(Kphi-Nr_ldpp(i,j)*h_ldpp(i,j));
aglt_ldpp(i,j)=(lf_ldpp(i,j)*sind(beta)-h_ldpp(i,j)...
    *tand(phi_ldpp(i,j)))/h_ldpp(i,j);
agltbc_ldpp(i,j)=(lf_ldpp(i,j)*sind(beta)-h_ldpp(i,j)...
    *tan(phi_ldpp(i,j)))/h_ldpp(i,j)-brg*sind(beta);
    end
end

for i = 1:length(brgplot)
phi_ldp1(1,9)=Nr_ldp(1,9)*ag_ldp1(1,9)*h_ldp(1,9)/...
    (Kphi-Nr_ldp(1,9)*h_ldp(1,9));
agltbcplot_ldp1(i)=(lf_ldp(1,9)*sind(beta)-y_ldp(1,9)*cosd(beta)...
    -h_ldp(1,9)*tan(phi))/h_ldp(1,9) - brgplot(i)*sind(beta);
phi_ldp2(1,9)=Nr_ldp(1,9)*ag_ldp2(1,9)*h_ldp(1,9)/...
    (Kphi-Nr_ldp(1,9)*h_ldp(1,9));
agltbcplot_ldp2(i)=(lf_ldp(1,9)*sind(beta)+y_ldp(1,9)*cosd(beta)...
    -h_ldp(1,9)*tan(phi))/h_ldp(1,9) - brgplot(i)*sind(beta);
phi_ldppl(9,9)=Nr_ldppl(9,9)*ag_ldppl(9,9)*h_ldppl(9,9)/...
    (Kphi-Nr_ldppl(9,9)*h_ldppl(9,9));
agltbcplot_ldppl(i)=(lf_ldppl(9,9)*sind(beta)-h_ldppl(9,9)...
    *tan(phi_ldppl(9,9)))/h_ldppl(9,9) - brgplot(i)*sind(beta);
phi=Nr_ld(9)*ag_ld(9)*h_ld(9)/(Kphi-Nr_ld(9)*h_ld(9));
agltbcplot_ld(i)=(lf_ld(9)*sind(beta)-h_ld(9)*tan(phi))/...
    h_ld(9) - brgplot(i)*sind(beta);
end

figure(6)
hold on
title('Braking while cornering')
xlabel('Cornering [g]')
ylabel('Braking [g]')
```

```
axis([0.3 0.8 0 0.5])
plot(agltbcplot_ldp1,brgplot,'g')
plot(agltbcplot_ldp2,brgplot,'b')
plot(agltbcplot_ldppl,brgplot,'r')
plot(agltbcplot_ld,brgplot,'.-')

%%---------------BRAKE DIMENSIONING, HYDRAULIC BRAKE SYSTEM----------------

g = 9.82;
Fh = 200;% [N] 93/14/EEC 2.1.4
L_hb = 0.1;%[m] leverage handbrake (service brake)
L_hmc = 0.025;%[m] leverage from handbrake to master cylinder
dmc = [0.014 0.01587 0.0175];% [m] diameter, master cylinder
dfc = [0.025 0.03 0.034 0.043];% [m] diameter, front caliper piston
drc = [0.025 0.03 0.034 0.043];% [m] diameter, rear caliper piston
r = [0.0625 0.0675 0.0725 0.0775 0.0825]; %[m] average radius for fbd
rr = [0.0625 0.0675 0.0725 0.0775 0.0825];%[m] average radius for rbd
npf = 2;                 %       number of pistons, total, front
npr = 4;                 %       number of pistons, total, rear
rw = 0.215;              % [m] radius wheel
mybd = 0.5;              %       friction coefficient brake disc
myroad = 1; % friction on road (tarmac)surface [dry]

for i = 1: length(dmc)
for j = 1:length(dfc)
% --------------Areas, mastercylinders and pistons
Amc(i) = (dmc(i)/2)^2*pi; %m^2
Afp(j) = npf*(dfc(j)/2)^2*pi; %m^2 total area front caliper pistons

%---------------Front brake system
Fmc = Fh*L_hb/L_hmc;
Pb(i) = Fmc/Amc(i);
Fb1(i,j) = Pb(i)*Afp(j);
Fbdf(i,j) = Fb1(i,j)*mybd;

for p = 1:length(r)
    Ff(i,j,p) = Fbdf(i,j)*r(p)/rw;
end

%---------------Rear brake system
for k = 1:length(drc)
Arp(k) = npr*(drc(k)/2)^2*pi; %m^2 total area front caliper pistons

Fb2(i,k) = Pb(i)*Arp(k);
Fbdr(i,k) = Fb2(i,k)*mybd;

        for q = 1:length(rr)
            Fr(i,k,q) = Fbdr(i,k)*rr(q)/rw;
        end
end

end
end

figure(1)
hold on
```

```
title('AVAILABLE BRAKEFORCE FROM HANDLE, FRONT')
xlabel('Diameter, front caliper piston [m]')
ylabel('Diameter, master cylinder [m]')
zlabel('Brakeforce [N]')
for i = 1:length(r)
mesh(dfc,dmc,Ff(:,:,i))
end

figure(2)
hold on
title('AVAILABLE BRAKEFORCE FROM HANDLE, REAR')
xlabel('Diameter, rear caliper piston [m]')
ylabel('Diameter, master cylinder [m]')
zlabel('Brakeforce [N]')
for i = 1:length(rr)
mesh(drc,dmc,Fr(:,:,i))
end

m = [225 385];
lf = [1.2 1.8];
h = [0.54 0.6];
a = [0:0.1:9];                  % [m/s^2] retardation
Ltot = 1.96;

    for i = 1:length(m)
        for j = 1:length(a)
            for k = length(myroad)
            Nf(i,j) = (m(i)*(g*(Ltot-lf(i))+a(j)*h(i)))/Ltot;
            Nr(i,j) = (m(i)*(g*lf(i)-a(j)*h(i)))/Ltot;

            Fbf(i,j) = Nf(i,j)*myroad;
            Fbr(i,j) = Nr(i,j)*myroad;
            end
        end
    end

% figure(3)
% hold on
% title('SYMMETRICAL LOAD')
% xlabel('Deceleration [m/s^2]')
% ylabel('Available brakeforce on road [N]')
% axis([0 length(a)/10 0 3000])
% plot(a,Fbf,'--')
% %plot(a,Fbr,'--')
%
% figure(4)
% hold on
% axis([0 3000 0 length(a)/10])
% plot(Fbr,a)


%%---------------DRUMBRAKE--------------------------------------------------
clear all

Fh = 200;%control force
Fc = Fh*[1 2 3 4 5 6]; %amplification
my = 0.6;%pad friction
```

```
D = [0.1:0.01:0.2];%drum diameter
rw = 0.215;%wheel radius

% phi2 = [70:5:95]*pi/180;
phi2 = 80*pi/180;
phi1 = 20*pi/180;

    Is = cos(phi1)-cos(phi2);
    Iss =(phi2-phi1)/2-(sin(2*phi2)-sin(2*phi1))/4;
    Isc = (cos(2*phi1)-cos(2*phi2))/4;

     for j = 1:length(D)
%          for k = 1:length(phi2)REMOVE TO GET VARIATIONS INTERVAL OF
% PHI1 AND PHI2
             for i = 1:length(Fc)
                 R(j) =D(j)/2;

% Is(k) = cos(phi1)-cos(phi2(k));
% Iss(k) =(phi2(k)-phi1)/2-(sin(2*phi2(k))-sin(2*phi1))/4;
% Isc(k) = (cos(2*phi1)-cos(2*phi2(k)))/4;

      L(j) = (R(j)*2)-R(j)*0.1;
      A(j) = (L(j)*1.05)/2;

%T(j,k,i)=(my*Is(k)*Fc(i)*L(j))/...
%((A(j)*Iss(k))/R(j)-my*Is(k)-(A(j)*Isc(k)/R(j)));
%
%Fb(j,k,i) = -2*T(j,k,i)/rw

T(j,i) = (my*Is*Fc(i)*L(j))/((A(j)*Iss)/R(j)-my*Is-(A(j)*Isc/R(j)));

Fb(j,i) = -2*T(j,i)/rw;
         end
%        end
end

% figure(1)
% hold on
% mesh(R,phi2,Fb(:,:,1))
% mesh(R,phi2,Fb(:,:,3))
% mesh(R,phi2,Fb(:,:,6))

figure(1)
plot(D,Fb)


%%---------------STOPPING DISTANCES-----------------------------------------
clc
%clf
clear all

% MAXLOAD 385 kg lf = 1.4 h = 0.6
% ONLY DRIVER lf = 1.2 h = 0.54

m = 280;            %kg
lf = 1.2;           %m
h = 0.54;           %m
```

```
Ltot = 1.96;          %m
lr =Ltot-lf;          %m
g = 9.82;             %m/s^2
my = 1;               %roadfriction

v0 = 36/3.6;          %m/s

t = [0:0.01:5];

af = 2.7; %m/s^2
ar = 2.7; %m/s^2

Ff = 1340; %brake force generated by specific brakesystem at Fh 200 N front
Fr = 2648; %brake force generated by specific brakesystem at Fh 200 N rear

Nf = (m*g*lr+m*af*h)/Ltot;
Nr = (m*g*lf-m*ar*h)/Ltot;

Bf = Nf*my;
Br = Nr*my;

Ffv = [0:Ff/40:Ff ones([1 460])*Ff];
Bfv = [0:Bf/40:Bf ones([1 460])*Bf];

Frv = [0:Fr/40:Fr ones([1 460])*Fr];
Brv = [0:Br/40:Br ones([1 460])*Br];

%ONLY FRONT
for i = 1:length(t)
    if Ff >= Bf
        aff(i) = Bfv(i)/m;
    else
        aff(i) = Ffv(i)/m;
    end
   vf(i) = v0 - aff(i)*t(i);

    if vf(i) <= 0
        vf(i)=0;
    end

    sf(i)= vf(i)*t(2);
    sf_tot = sum(sf);
end
sf_tot

%ONLY REAR
for i = 1:length(t)
    if Fr >= Br
        arr(i) = Brv(i)/m;
    else
        arr(i) = Frv(i)/m;
    end
   vr(i) = v0 - arr(i)*t(i);

    if vr(i) <= 0
        vr(i)=0;
```

```
        end

        sr(i)= vr(i)*t(2);
        sr_tot = sum(sr);
end
sr_tot

ac = 4.4; %m/s^2

Nfc = (m*g*lr+m*ac*h)/Ltot;
Nrc = (m*g*lf-m*ac*h)/Ltot;

Bfc = Nfc*my
Brc = Nrc*my

Bfcv = [0:Bfc/40:Bfc ones([1 460])*Bfc];
Brcv = [0:Brc/40:Brc ones([1 460])*Brc];

%COMBINED
for i = 1:length(t)
        if Fr >= Brc & Ff>=Bfc
                acc(i) = (Bfcv(i)+Brcv(i))/m;
        elseif Fr >=Brc & Ff<Bfc
                acc(i) = (Brcv(i)+Ffv(i))/m;
        elseif Fr<Brc & Ff>=Bfc
                acc(i) = (Frv(i)+Bfcv(i))/m;
        else
                acc(i) = (Ffv(i)+Fr(v))/m;
        end
      vc(i) = v0 - acc(i)*t(i);

        if vc(i) <= 0
                vc(i)=0;
        end

        sc(i)= vc(i)*t(2);
        sc_tot = sum(sc);
end
sc_tot

%ELECTRIC BRAKING
E0 = (m*v0^2)/2
Eb = 5000;

for i = 1:length(t)
        Er(i) = E0-Eb*t(i);

        if Er(i)<= 0
                Er(i) = 0;
        end

        ve(i) = sqrt((Er(i)*2)/m);

        se(i) = ve(i)*t(2);
        se_tot = sum(se);
end
```

```
se_tot

%%----------------FORCES ON BODY
clc
% clf
clear all

g = 2.5*9.82;
a = 0.035; %distance from floor to swingarm axis
my = 1; %road friction
rw = 0.215;%wheel radius

%curbweight = 160 Nr = 375
%weight with driver = 235 Nr = 683.3
%maxweight = 385 Nr = 1165
%genomslag = 2.5*385 Nr = 2911

mtot = 385-26.5*2;

ay = 9.82*0.5;

Nr = mtot*g*0.5*(1.4/1.96);
Fwy = mtot*ay*my;

sh = 0.22;%vertical distance, swingarm axis to upper damper mount
sd = 0.144;%longitudinal distance, swingarm axis to upper damper mount
Ls = 0.4;%longitudinal distance, swingarm axis to wheel axis
Lfs = [0.16:0.01:0.4];%longitudinal distance,swingarm axis to lower damper
%                     mount
h = [-0.06:0.005:0.06];%vertical distance between swingarma axis and
%                      lower damper mount
w = [0.055:0.005:0.175];%lateral displacement of lower damper mount

gamma = 7;
eta = 6;

for k = 1:length(h)
        for j = 1:length(w)
            for i =1:length(Lfs)
alpha(i,k) = atand((sh-h(k))/(Lfs(i)-sd));

Fs(i,k) = Nr*Ls/(sind(alpha(i,k))*Lfs(i)+cosd(alpha(i,k))*h(k));

Flmx(i,k) = Fs(i,k)*cosd(alpha(i,k));

Fumx(i,k) = -Fs(i,k)*sind(90-alpha(i,k));

Flmz(i,k) = Fs(i,k)*sind(alpha(i,k))-Nr;

Fumz(i,k) = Flmz(i,k)+Nr;

Flmy(i,k) = -Fwy;

Fs(i,k) = sqrt(Flmx(i,k)^2+(Flmz(i,k))^2);

Mxy(i,j,k) = Fwy*Ls-Flmx(i,k)*w(j);
```

```
Myz(i,j,k) = Fwy*rw-(Flmz(i,k))*w(j);

su(i,k) = Lfs(i)*sind(gamma)+h(k)*cos(gamma);
so(i,k) = Lfs(i)*sind(eta)-h(k)*cosd(eta);

lu(i,k) = Lfs(i)*cosd(gamma)-sd;
lo(i,k) = Lfs(i)*cosd(eta)-sd+h(k)*sind(eta);

sv(i,k) = sh+su(i,k);

sl1(i,k) = sqrt(sv(i,k)^2+lu(i,k)^2);
sl2(i,k) = sqrt((sh-so(i,k))^2+lo(i,k)^2);

stroke(i,k) = sl1(i,k)-sl2(i,k);

cl = rw+Ls*sind(gamma)-a; %ground clearance

    if sl1(i,k) < 0.28 | sl1(i,k) > 0.31
        sl1(i,k) = 0;
        stroke(i,k) = 0;
    end

    if stroke(i,k) < 0.05 | stroke(i,k) > 0.1
        sl1(i,k) = 0;
        stroke(i,k) = 0;
    end

    if w(i) < 0.095 & Lfs(i) > 0.310
        sl1(i,k) = 0;
        stroke(i,k) = 0;
    end

    if cl < 0.15 | cl > 0.23
        sl1(i,k) = 0;
        stroke(i,k) = 0;
    end

    if Flmx(i,k) > 3000 | Fumz > 3000
        sl1(i,k) = 0;
        stroke(i,k) = 0;
    end
            end
        end
end

figure(1)
hold on
title('FORCE IN X-DIR, SWINGARM MOUNT')
xlabel('Distance from rear swing-axle [m]')
ylabel('Height difference from wheelcenter [m]')
zlabel('Force [N]')
 mesh(Lfs,h,Flmx)
%mesh(Lfs,h,Fumx)

figure(2)
```

```
hold on
title('FORCE IN Z-DIR, SWINGARM MOUNT')
xlabel('Distance from rear swing-axle [m]')
ylabel('Height difference from wheelcenter [m]')
zlabel('Force [N]')
% mesh(Lfs,h,Flmz)
mesh(Lfs,h,Flmz)

% for i = 1:length(Lfs)
figure(3)
hold on
title('TORQUE M X Y ')
xlabel('Height difference from wheelcenter [m]')
ylabel('Distance from trackwidth centerline [m]')
zlabel('Torque [Nm]')
mesh(h,w,Mxy(:,:,13))

figure(4)
hold on
title('TORQUE M Y Z')
xlabel('Height difference from wheelcenter [m]')
ylabel('Distance from trackwidth centerline [m]')
zlabel('Torque [Nm]')
mesh(h,w,Myz(:,:,13))
% end

figure(5)
hold on
title('STROKE')
xlabel('Distance from rear swing-axle [m]')
ylabel('Height difference from wheelcenter [m]')
zlabel('Stroke [m]')
mesh(Lfs,h,stroke)

figure(6)
hold on
title('FREE-LENGTH')
xlabel('Distance from rear swing-axle [m]')
ylabel('Height difference from wheelcenter [m]')
zlabel('Free-lenght [m]')
mesh(Lfs,h,sl1)
```